

CONFIDENTIAL

FP7-ICT Future Networks
SPECIFIC TARGETTED RESEARCH PROJECT
Project Deliverable

PHYDYAS Doc. Number	PHYDYAS_013
Project Number	ICT - 211887
Project Acronym+Title	PHYDYAS – PHYsical layer for DYnamic AccesS and cognitive radio
Deliverable Nature	Report
Deliverable Number	D7.1
Contractual Delivery Date	July 1 st , 2009
Actual Delivery Date	July 29 th , 2009
Title of Deliverable	Compatibility of OFDM and FBMC systems and reconfigurability of terminals
Contributing Workpackage	WP7
Project starting date; Duration	01/01/2008; 30 months
Dissemination Level	CO
Author(s)	Frank Schaich (ALUD), Vidar Ringset (SINTEF), Maurice Bellanger, Haijian Zhang, Didier Le Ruyet (CNAM)

Abstract: This deliverable motivates the need of compatibility of the physical layer proposed in PHYDYAS to a state-of-the-art OFDM based physical layer. The way used to guarantee maximal compatibility is presented. The base version of the physical layer enhanced in PHYDYAS is depicted. Necessary adjustments to evolve it to FBMC mode are given. Additional adjustments sacrificing compatibility to some extent to improve the performance are proposed and the performance gain assessed. Compatibility at initialization is treated in more detail. Here, the memory preloading technique is presented. A way to distinguish between OFDM and FBMC signals is proposed and its performance assessed. Finally reconfigurability of the transmitters/receivers, especially under the view of the demonstrator developed in D9, is examined.

Contents

1	INTRODUCTION	3
2	OFDM BASED PHYSICAL LAYER EVOLVED IN PHYDYAS	4
3	EVOLVING THE PHYSICAL LAYER TO FBMC MODE	6
3.1	From OFDM to FBMC	6
3.2	Improving the performance of the new physical layer	11
4	COMPATIBILITY AT INITIALIZATION	28
4.1	The memory preloading technique.....	28
4.2	Cascading preamble and data in OQAM modulation.....	31
4.3	Transmission parameter estimation.....	33
4.4	Memory preloading with MIMO.....	36
4.5	Estimation in the cognitive radio context	38
4.6	Conclusion and recommendations.....	39
5	AUTOMATIC DETECTION OF OFDM / FBMC	40
6	RECONFIGURABILITY	47
7	REFERENCES	52

1 Introduction

The objective of PHYDYAS is to propose a physical layer for future radio systems that is more efficient than the present OFDM (Orthogonal Frequency Division Multiplexing) physical layer and better suited to the new concepts of DASM (Dynamic Access Spectrum Management) and cognitive radio. The fundamental change is the replacement of the OFDM with a multicarrier system based on filter banks (filter bank based multi carrier, FBMC).

The move from an existing physical layer to a new one requires a certain degree of acceptance and common understanding within the community. This acceptance nowadays is inalienable to successfully promote the new physical layer. To reach this acceptance the community has to be convinced of the gains the new physical layer provides. Performance improvement naturally is one of these gains. However, to assure that the new physical layer may become reality, further aspects need to be considered:

- **Easy migration**
The migration from existing transmission schemes must be not too complex and expensive to be realized by involved groups (provider, standardization community).
- **Easy legacy support**
The replaced physical layer should still be supported at least for some time, to reach a smooth transition, both for the consumer and the provider.
- **Cheap dual mode terminals**
Once a new physical layer is accepted by the community and even first deployments are on their way, already deployed ones based on OFDM surely won't be shutdown instantly. Thus dual mode terminals operating in both network types are feasible.
- **Easy comparability**
To convince the community of the achievable gains, the new physical layer has to be comparable to existing solutions in terms of complexity and performance.

All these preconditions suggest to aim for as much compatibility to existing solutions as possible without trading to much performance.

This work package somehow differs from the others. Its main target is not to provide an algorithmic investigation of a specific part of the new physical layer. Instead its role is to assure that the preconditions mentioned above are considered. Basically the work package is split into four parts:

- compatibility at specification and system parameter level
- compatibility at the initialization phase
- techniques and algorithms to automatically identify OFDM and FBMC signals
- reconfigurability of terminals in hardware and software

This deliverable is structured as follows: The second chapter recapitulates the actions taken to reach a common basis within the consortium with respect to the base version of the transmission system

studied in PHYDYAS. The common ground of the FBMC solution and the OFDM based physical layer taken as reference here is depicted (WiMAX was decided to be that reference system). Then, the necessary adjustments to evolve this base version to the FBMC solution are described. Further possible adaptations, not necessarily crucial for the fundamental operation, but leading to an improved performance, are next. This way a multitude of solutions varying in terms of compatibility and performance are available. Next are the investigations performed regarding the compatibility at the initialization phase. Afterwards the techniques for identification are presented. Finally the reconfigurability of the terminals in hardware and software is assessed.

2 OFDM based physical layer evolved in PHYDYAS

At the preparation of the project it was decided to integrate the algorithms and structures investigated in PHYDYAS into a state-of-the-art OFDM-based system (WiMAX was chosen). Thus, at the first semester of the project the main task of this work package was to introduce WiMAX and its components/behaviour to the consortium. This way the algorithms and structures developed in PHYDYAS can use WiMAX as a starting point and the target of high compatibility can be easier guaranteed. To introduce WiMAX to the consortium several documents were produced and distributed:

- WiMAX forum channel models [1]
This document was intended to harmonize the used channel models of all partners and to guarantee the use of models accepted within the community. This is important to gain acceptance.
 - WiMAX system profile [2]
Basic parameters and configuration of WiMAX were introduced here (access scheme, frame parameters, data processing schemes ...). Again the target of this document was to give the consortium a point to start with.
 - Framing in WiMAX [3]
More details about the frame structures are included here. Subchannelization schemes and pilot placement were the core elements.
 - Simulator settings [4]
First general decisions made on the simulator were disseminated here.
 - Ranging/network entry in WiMAX [5]
As synchronization is a major theme in PHYDYAS this document delivers an overview about initial and periodic ranging (the synchronization mechanisms used in WiMAX).
 - Residual timing error [6]
A more detailed view to timing synchronization in WiMAX is given. Especially the tolerances to be met are included.
-

- Frequency offset [7]
Similar to the former document now for the carrier offset.
- MIMO in WiMAX [8]
This document gives an overview about MIMO modes used in WiMAX.
- Channel estimation [9]
The way channel estimation is done within the simulator (for the WiMAX case) is described here.
- From WiMAX to FBMC [10]
The WiMAX version of the simulator was finalized at the date of this document. Thus, the needed actions to include the FBMC solution into the simulator are depicted here. Especially the mapping to the different work packages is included.
- Preamble and sounding zone [11]
A further look into the use of preambles and sounding zones in WiMAX is given here. This document especially was targeted to inform the partners working on preamble based estimation/synchronization about the tools WiMAX provides.
- Burst allocation in WiMAX [12]
Burst allocation in WiMAX downlink significantly differs from that in WiMAX uplink. This document was intended to describe the respective schemes to the work package dedicated to scheduling.

The basic system parameters of the physical layer to be evolved are chosen as follows:

Table 1: System parameters

Parameter name	value
number of subcarriers	1024
carrier frequency	2.5 GHz
bandwidth	10 MHz
sampling rate	11.2 MHz
subcarrier spacing	10.94 kHz
normalized length of cyclic prefix	1/8
frame length	5 ms
coding scheme	CTC
code rate	1/2
number of turbo iterations	4

3 Evolving the physical layer to FBMC mode

The adjustments done to the physical layer used as base (WiMAX) are twofold. On the one hand there are the necessary changes, to evolve the OFDM based physical layer to the solution proposed by PHYDYAS. The next chapter describes these adjustments. Afterwards further adjustments to improve the performance are presented.

3.1 From OFDM to FBMC

Figure 1 illustrates the necessary adjustments to the transmitter to implement the FBMC mode (White blocks are common to both modes, blue ones are FBMC specific, orange ones OFDM specific. Green blocks indicate structures needed in both modes, however, differing in implementation):

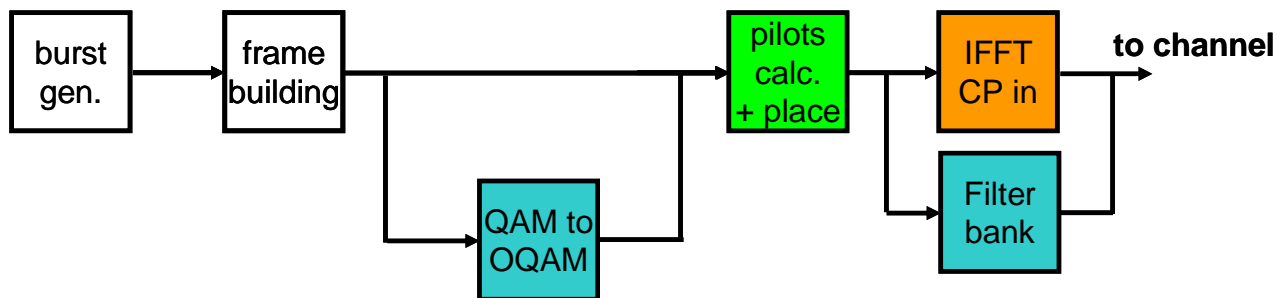


Figure 1: Transmitter including FBMC mode

Burst generation includes the bit source, forward error coding and symbol mapping. In the multi-user case several bursts are generated.

The frame builder generates the frames to be transmitted including the user bursts and the preamble (in DL). These two blocks are common between OFDM and FBMC mode. No adjustments are necessary here, as the methods used in WiMAX are applicable to the physical layer investigated in PHYDYAS. Naturally adjustments may be viable; however, at this point just necessary adjustments are included.

The first addition is the OQAM block. He is specific to the FBMC mode. In OFDM mode it gets bypassed.

Pilots are needed in both modes. However, their calculation differs. In OFDM pilots are simple BPSK symbols. In FBMC pilot processing is a bit more complicated. As channel coefficients typically are complex (in baseband notation) the interference caused by adjacent data symbols would disturb channel estimation. To solve this matter the auxiliary pilot method is used in PHYDYAS [13] to cancel this interference.

Once the frame is completed signal generation is triggered. In OFDM mode IFFT and the insertion of the cyclic prefix do the job, in FBMC mode the synthesis filter bank is invoked. Here the most significant adaptation is necessary.

Figure 2: Receiver including FBMC mode depicts the necessary adjustments to the receiver to implement the FBMC mode (White blocks are common to both modes, blue ones are FBMC specific, orange ones OFDM specific. Green blocks indicate structures needed in both modes, however, differing in implementation):

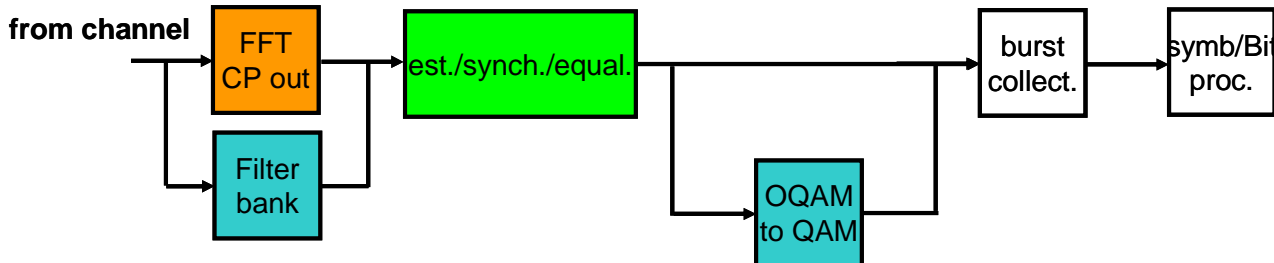


Figure 2: Receiver including FBMC mode

Corresponding to the signal generation at the transmitter the received signal get's transformed using a FFT after the removal of the cyclic prefix, if OFDM mode is active. In FBMC mode the analysis filter bank does the transformation.

Channel estimation, synchronization and equalization are required in both modes, differing in their implementation [13][14][15].

Only in FBMC mode the conversion from OQAM to QAM symbols is needed. In OFDM mode this block gets bypassed.

Burst collection and symbol/Bit processing again are common to both modes.

The move from the existing physical layer using OFDM to a mixed physical layer using both OFDM and FBMC require some changes. In PHYDYAS WiMAX was chosen as the reference system and the differences between the two systems have been identified. The envisaged use of FBMC in a network is that stations capable of doing FBMC should also be capable of doing OFDM, i.e. dual mode terminals at least in a transition period. This will ensure backward compatibility with legacy systems and ease a migration toward use of FBMC. In case a BS is capable of doing FBMC, certain zones within the frame can be allocated for FBMC if there are associated MS capable of doing FBMC. The FBMC stations are associated in the network using the normal procedures used by other OFDM stations. Initial ranging is done as for OFDM. In addition they describe their FBMC capabilities to the BS. The BS allocates a special zone to the FBMC stations, preferable at the end of the uplink or downlink frames. The reason for having at the end is to minimize the disturbance for the OFDM stations, which will not be able to demodulate the FBMC signals. Another reason is to minimize the overhead since FBMC requires a time gap between the OFDM and FBMC zones. The TTG and RTG gaps between downlink and uplink can be utilized as the gap on one side.

A dual mode transmitter is being built in WP9 and the main differences between OFDM stations and FBMC stations on the transmitter's physical layer are listed below.

Downlink PUSC without segmentation:

In downlink PUSC the pilot pattern within a cluster is as shown in Figure 3a). The cluster size is 14 (in frequency) x 2 (in time). A similar cluster structure can be used for FBMC as shown in Figure 3 b). However, in order to ease the calculation of the auxiliary pilots a modified pilot position scheme is preferred as shown in Figure 3c). Data subcarriers to each MS is scattered in different clusters along the frequency axis. In WiMAX there is room for 30 subchannels along the frequency axis using 840 carriers (including pilots). Due to the better attenuation of the out-of-band signal when

using a filterbank, more carriers at the band edges can be used for data transmission. Maximally, 912 subcarriers can be fitted into the 10 MHz bandwidth. With constraint that there shall be an integer number of subchannels along the frequency axis, the maximum number of usable carriers is 896 (including pilots). This results in 32 subchannels along the frequency axis. The allocation scheme for WiMAX and FBMC will therefore be different since FBMC have to support a larger number of subcarriers, but it does not necessary lead to any big changes. A WiMAX station has to support different allocation schemes in any case and the FBMC allocation scheme will just be another one. This applies both to the logical and physical allocations.

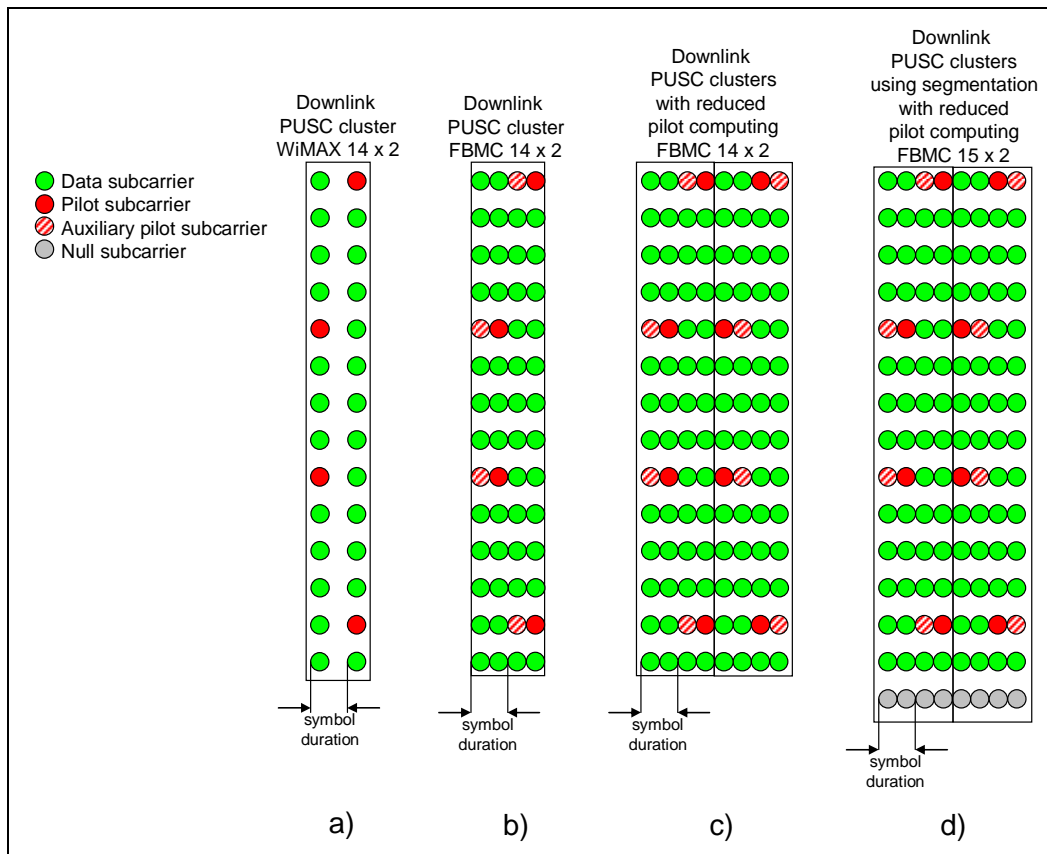


Figure 3: Downlink PUSC

Downlink PUSC with segmentation.

For downlink PUSC with segmentation the physical assignment of clusters belonging to one segment are scattered over the entire frequency range. It is assumed that the radiated signal in different segments are not phase coherent which means that a frequency gap of one carrier is required between the clusters. The cluster size for WiMAX is 14 (in frequency) x 2 (in time) subcarriers. Using a cluster size of 15 (in frequency) x 2 (in time) for FBMC allows for one empty carrier between the slots and 30 subcarriers along the frequency axis using 900 active carriers, ref Figure 3 d). This is exactly the same as for WiMAX. The resulting increase in efficiency comes from removal of the guard interval which is up to 12.5%.

Uplink PUSC

Uplink PUSC is a particularly difficult case for FBMC. A guard subcarrier needs to be inserted between every pair of adjacent tiles, which are always allocated to different users. Furthermore, due to slot rotation, different users are allocated to consecutive tiles in the time direction.

The tile size for WiMAX is 4 (in frequency) x 3 (in time) subcarriers containing 8 data carriers and 4 pilot carriers, ref Figure 4 a). A slot is 6 tiles (24 in frequency x 3 in time subcarriers). The number of slots along the frequency axis is 35 for WiMAX.

Using the same tile size in FBMC would result in excessive overhead due to guard subcarriers and time gaps. The overheads can be reduced by increasing the tile size in either or both directions, or by dropping slot rotation. These changes would effect on frequency diversity due to smaller number of tiles and/or less effective slot rotation. Also the tradeoffs between frequency diversity and granularity of data rates would become more critical. Figure 4 b) and c) shows two alternatives for uplink PUSC; without slot rotation (5 x 3) and with slot rotation (5 x 6) where the pilot density is similar to that of WiMAX.

In WiMAX there is room for 35 slots along the frequency axis using 840 carriers. In FBMC the corresponding number is 30 both with and without slot rotation. This results in a capacity loss of 14.3%. The gain in capacity by omitting the cyclic prefix is equal or less than 12.5% and depends on the number of OFDM symbols used. The resulting capacity loss for FBMC over WiMAX on uplink PUSC is therefore at least of 1.8% (14.3% – 12.5%).

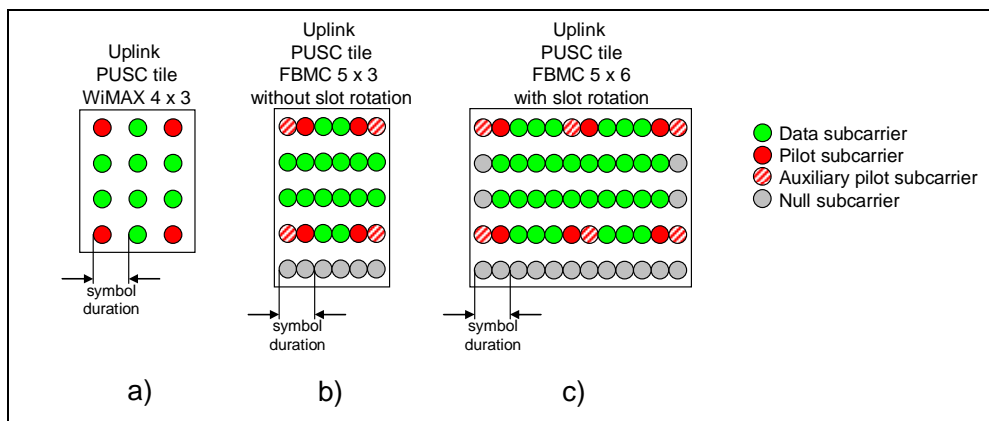


Figure 4: Uplink PUSC allocations for WiMAX and FBMC

AMC

For downlink AMC the same slot size can be used for WiMAX and FBMC, ref Figure 5 a) and b). Due to more usable carriers for FBMC the number of slots along the frequency axis can be increased from 48 (WiMAX) to 50. This, combined with the omission of the cyclic prefix, results in an increased capacity of 17.2% ($50/48 * 9/8 * 100\%$)

In the uplink AMC23, the main modification is to add guard subcarriers. Assuming static allocation of subcarriers to slots, this would necessitate the use of 19 subcarriers for each slot. If two adjacent slots are allocated to a single user over the whole AMC zone, the guard subcarrier in between is not necessary. However, to be able to utilize this possibility, the subcarrier allocation to slots would depend on scheduling, which is probably not practical. Therefore, the use of 19 subcarriers per slot is assumed, and the pilot pattern follows Figure 5 c). If the allocation of slots along the time axis belongs to different users within an AMC zone it probably most efficient to insert an empty slot between the users in order to maintain the regular frame and pilot structure. The number of slots

along the frequency axis in this case is exactly the same as for WMAX. Increased capacity for FBMC over WiMAX comes from removal of cyclic prefix which is equal or less than 12.5%

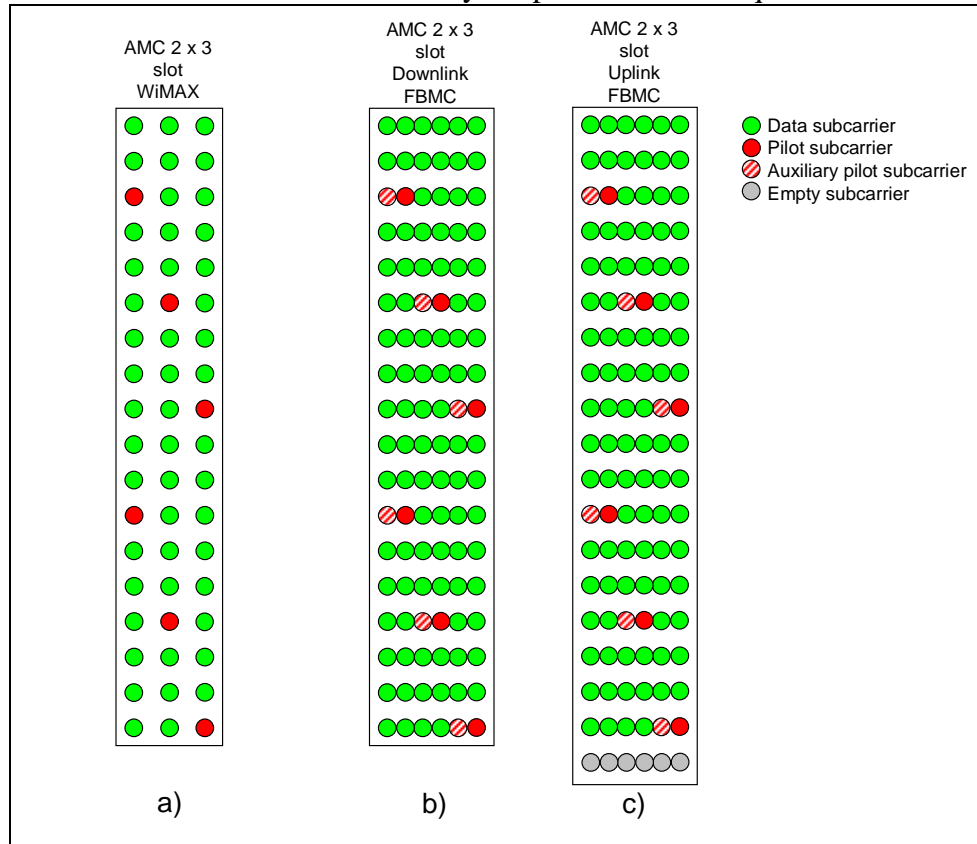


Figure 5: AMC allocations for AMC

Modulation

The same modulation types are used for WiMAX and FBMC, i.e. QPSK, 16QAM and 64QAM. The difference is that FBMC uses offset QAM modulation. This requires some preprocessing of the signal in front of the IFFT. Corresponding processing in the receiver is also required.

Pilots

The pilots in WiMAX are data independent. The position and value of the transmitted pilots are known at the receiver. Simple estimation of the received pilot amplitude and phase yields estimates for the channel's amplitude and phase for that frequency bin.

This is not the case for FBMC. Here the concept of auxiliary pilots is used. In this approach, a pilot consists of the main pilot and auxiliary pilot, which together correspond to one modulated OQAM symbol. Adjusting the primary part of the auxiliary pilot depending on the surrounding data symbols, the secondary part of the main pilot can be forced to take any desired value. For example the secondary part of the main pilot can be forced to be zero. Utilising this idea, pilots can be used in a similar way as in OFDM.

Since the value of the auxiliary pilot depends on the surrounding data some processing is required after the physical mapping of the data for calculation of the auxiliary pilots. In addition the offset QAM also requires a phase rotation of the signal in front of the IFFT. This block is an additional function for FBMC compared to WiMAX.

IFFT

FBMC is using the same IFFT size but it computes output signals at twice the speed compared to OFDM. FBMC produces two output vectors from the IFFT per “OFDM symbol”

Filterbank

This function is used only for FBMC. The filterbank consists of a polyphase filter with a structure as shown in Figure 6. The filterbank shown in this figure spans four symbols. The computational complexity of the filterbank is in the order of four multiplication and four additions per output sample. In addition memory for storing seven sets of output data from the IFFT is required.

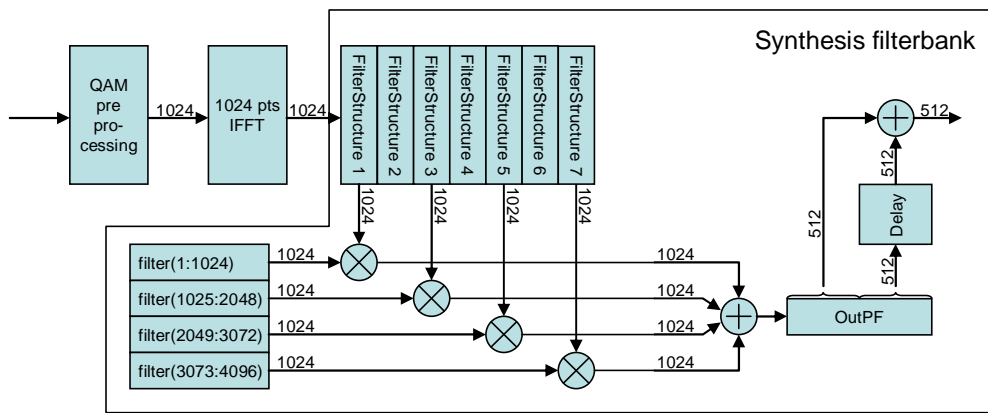


Figure 6: FBMC filterbank

Cyclic prefix

Adding the cyclic prefix is done by copying the last 1/8 of the OFDM symbol to the start of the symbol resulting in an OFDM symbol containing 9/8 times the number of samples of the original. Cyclic prefix is not used only for OFDM, not for FBMC.

Windowing

Multiplication by a window function might be required in the uplink direction at the borders between different users. This function is placed in the time domain after the filterbank. The first and last samples are multiplied by a smooth window function. This applies both to the transmitter and receiver.

3.2 Improving the performance of the new physical layer

One of the good features using FBMC is that it is a powerful tool for introduction of DASM. In order to compare the performance of OFDM and FBMC, WiMAX was chosen as a reference system. Better usage of carriers at the band edges and omission of the guard interval leads to increased spectral efficiency for FBMC compared to OFDM. The ability to suppress adjacent interferers will increase the efficiency of the FBMC system further in a dynamic spectrum management situation.

In order to keep compatibility with WiMAX the FBMC especially the uplink PUSC suffers from a loss in capacity. The reason for that is that the pilot pattern and density is kept as similar to WiMAX as possible. A further restriction is that the number of data carriers within a slot is always 48 for WiMAX. If this restriction is not imposed on the FBMC it is possible to have larger tile sizes. This might affect the frequency diversity gain for allocations using small FEC blocks. Under the assumption that the messages are fairly long, large FEC blocks can be used which will spread the message over the entire allocated bandwidth. This should then assure that the diversity gain is maintained even for larger tile sizes. Another way to increase the diversity gain without changing the basic allocation patterns is discussed later within this chapter.

Further gain in capacity can be achieved by allowing changed pilot pattern. Less dense pilots can be used. In the receiver the synchronization can be based on preamble and data aided methods combined with estimations based on pilots.

The basic parameters of a multicarrier system are the overall bandwidth, the number of subcarriers, the subcarrier spacing and the symbol length (naturally these parameters are depending on each other). A more detailed investigation worth are the subcarrier spacing and the respective symbol length. Their choice has several impacts to the signal transmission.

In basestation ruled networks (such as WiMAX) synchronization is mainly done by measuring the offsets (both frequency and timing) within the basestation and appropriate messaging, increasing the signalling overhead. Mobiles are not allowed to transmit data until defined accuracies are met, leading to higher latencies.

The system under investigation within PHYDYAS is designed with increased spectral efficiency and lowered latency in mind. By using reduced messaging between the basestation and the mobiles efficiency is increased, latency is lowered. Therefore a major point in PHYDYAS is synchronization by dedicated algorithms at the receiver. To perform timing synchronization within the receiver multi-tap equalizers are needed. With multi-tap equalizers a given amount of frequency selectivity within the range of a single subcarrier can be tolerated. Thus, broader subcarrier spacings may be adequate.

Table 2: General settings

link type	downlink
filter type	original CNAM version
K (overlapping factor)	4
pilot method	auxiliary pilots
pilot boost	2.5 dB (aux. pilot + main pilot)
excess ratio (burst truncation)	1
raised cosine ratio (burst truncation)	0.1
permutation mode	AMC23
modulation	16 QAM
FEC	CTC, code rate 1/2, 4 iterations
packet size	64 Bytes

Subcarrier spacings under investigation: 10.94 kHz (= WiMAX spacing), 21.88 kHz, 43.76 kHz and 87.52 kHz.

Burst placement is done in that way, that for any spacing the burst spans the same frequency/time range. Burst dimensions in number of subchannels/slots are adjusted accordingly:

downlink subframe

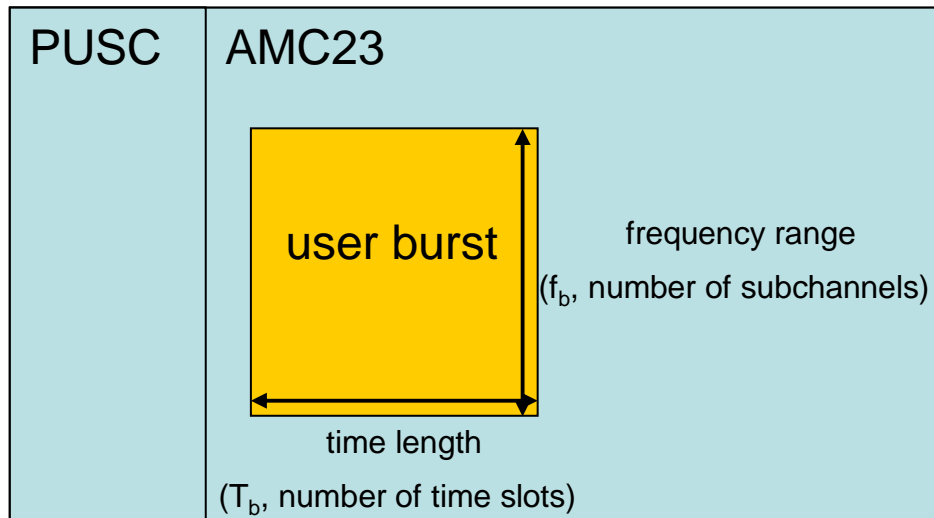


Figure 7: user burst placement

T_b and f_b are kept constant ($T_b = 0.274$ ms, $f_b = 6.1$ MHz). Thus, the number of time slots and the number of subchannels allocated depend on the subcarrier spacing:

Table 3: Allocation dimensions

subcarrier spacing	number of time slots / number of subchannels
10.94 kHz	1/32
21.88 kHz	2/16
43.76 kHz	4/8
87.52 kHz	8/4

First perfect channel knowledge is assumed. No frequency / timing offsets (beside Doppler) are present. Diverse equalization strategies (zero forcing with 1 and 3 taps, MSE with 3 taps) and diverse channel models (Ped B 3 km/h, Veh A 60 km/h and Veh B 60 km/h) are investigated:

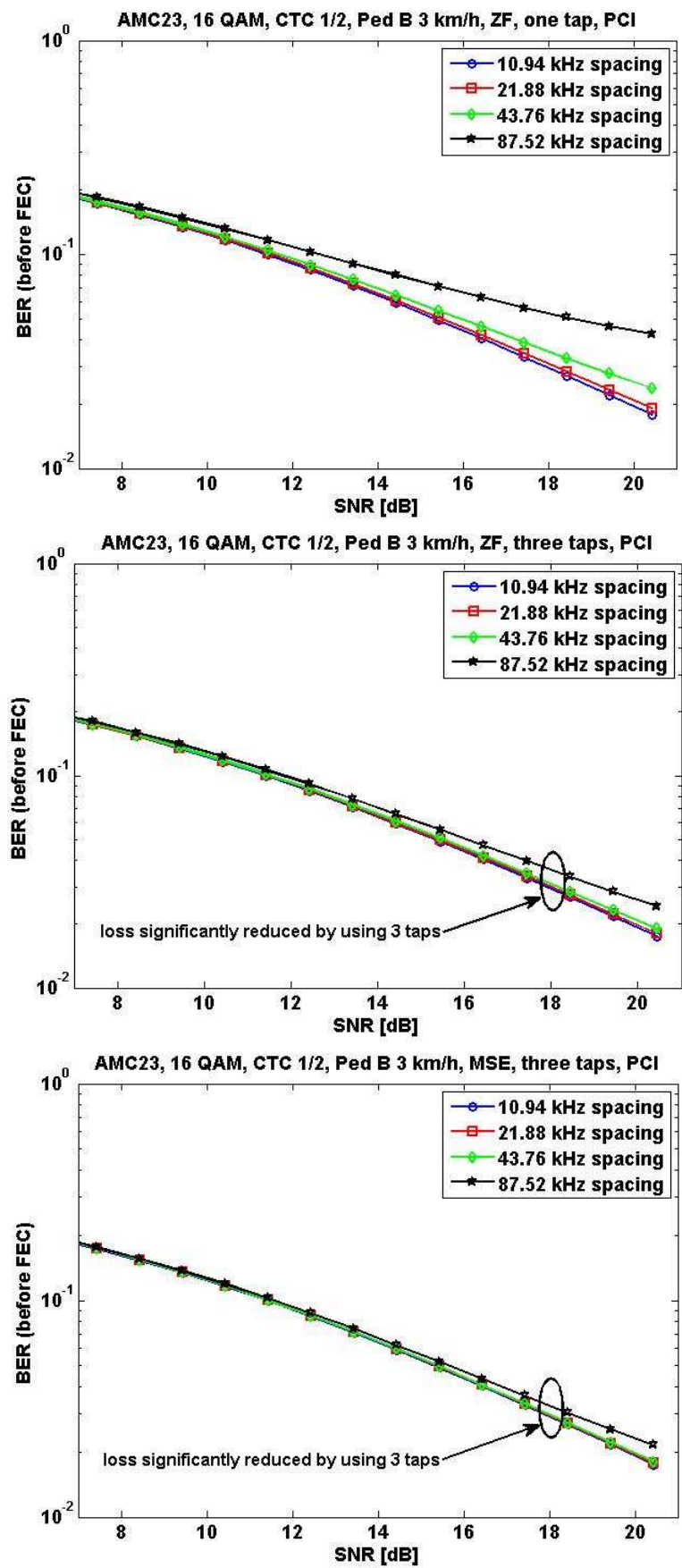


Figure 8: BER performance (before FEC) for different equalization strategies (Ped B 3 km/h)

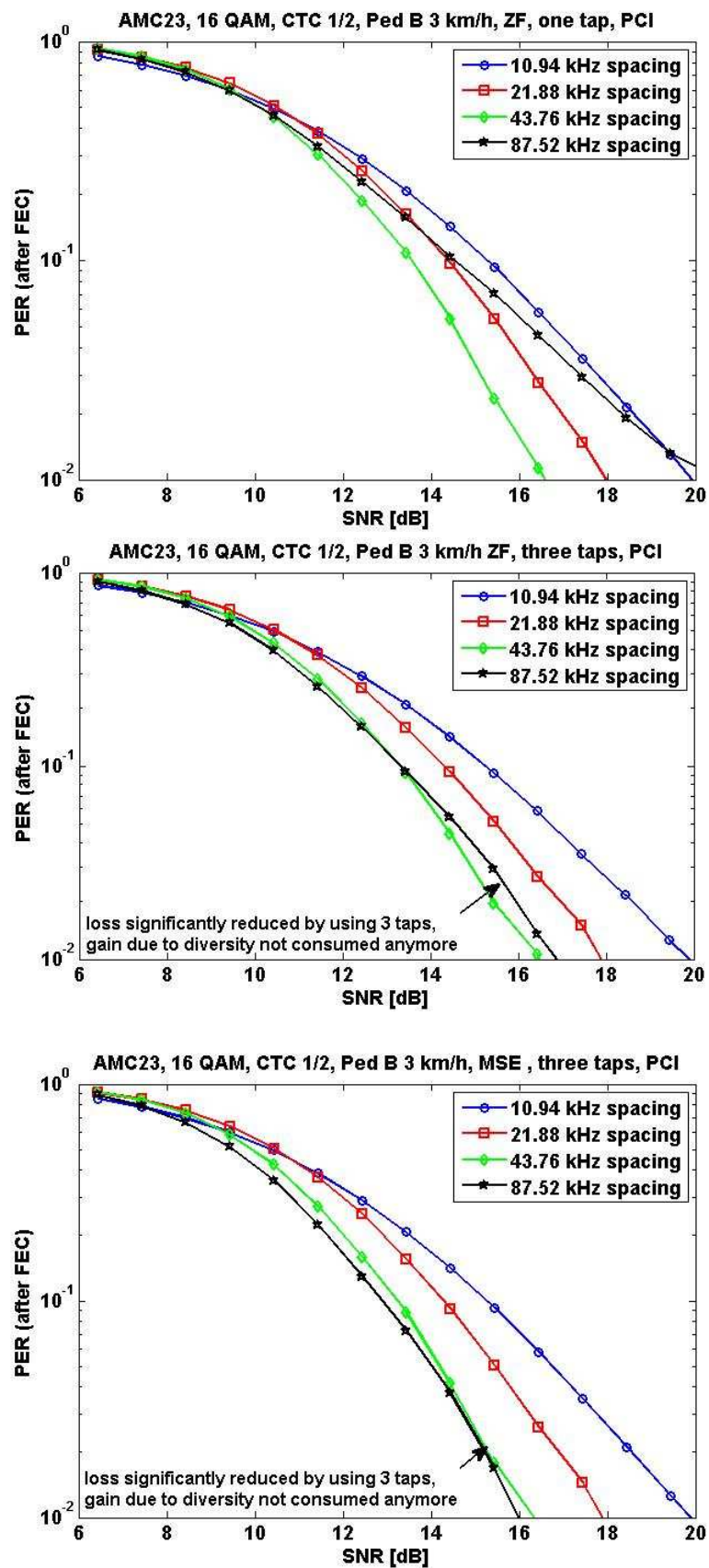


Figure 9: PER performance (after FEC) for different equalization strategies (Ped B 3 km/h)

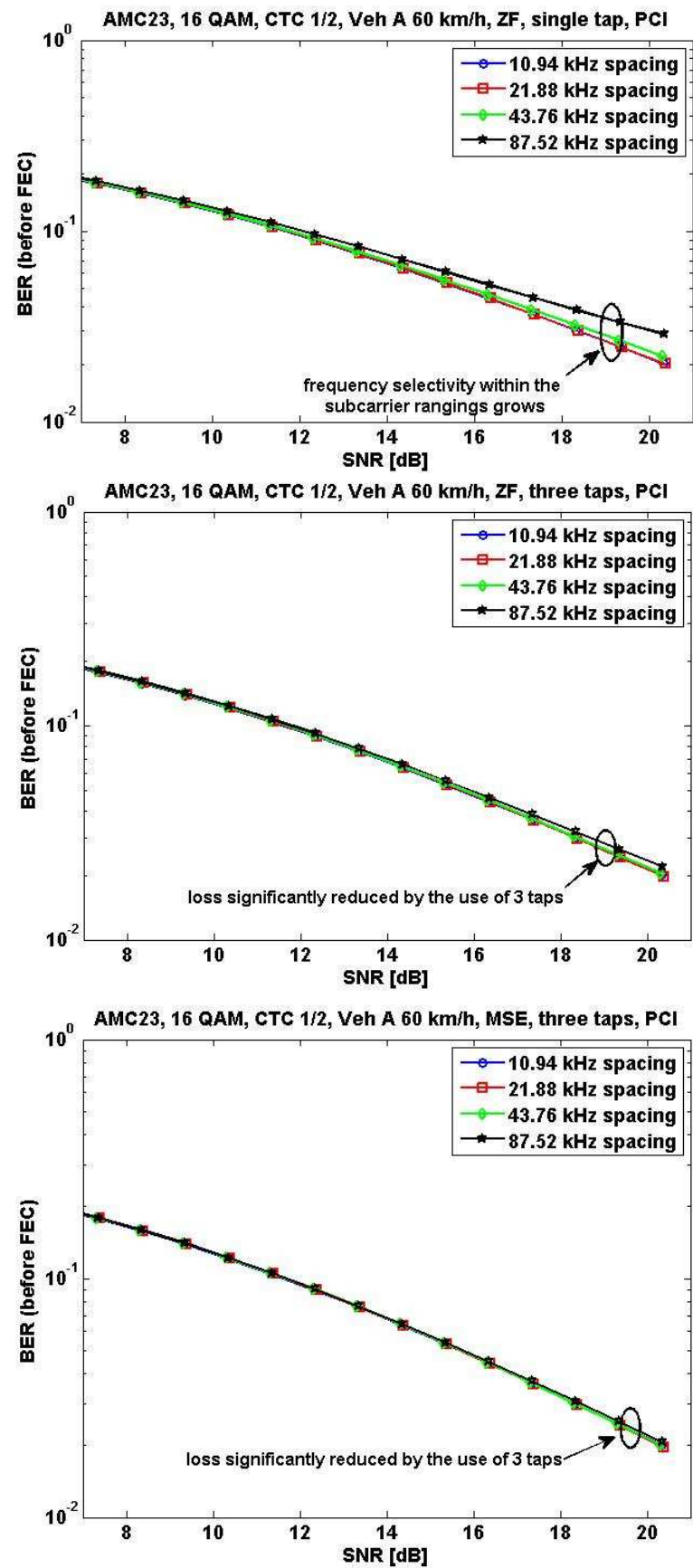


Figure 10: BER performance (before FEC) for different equalization strategies (Veh A 60 km/h)

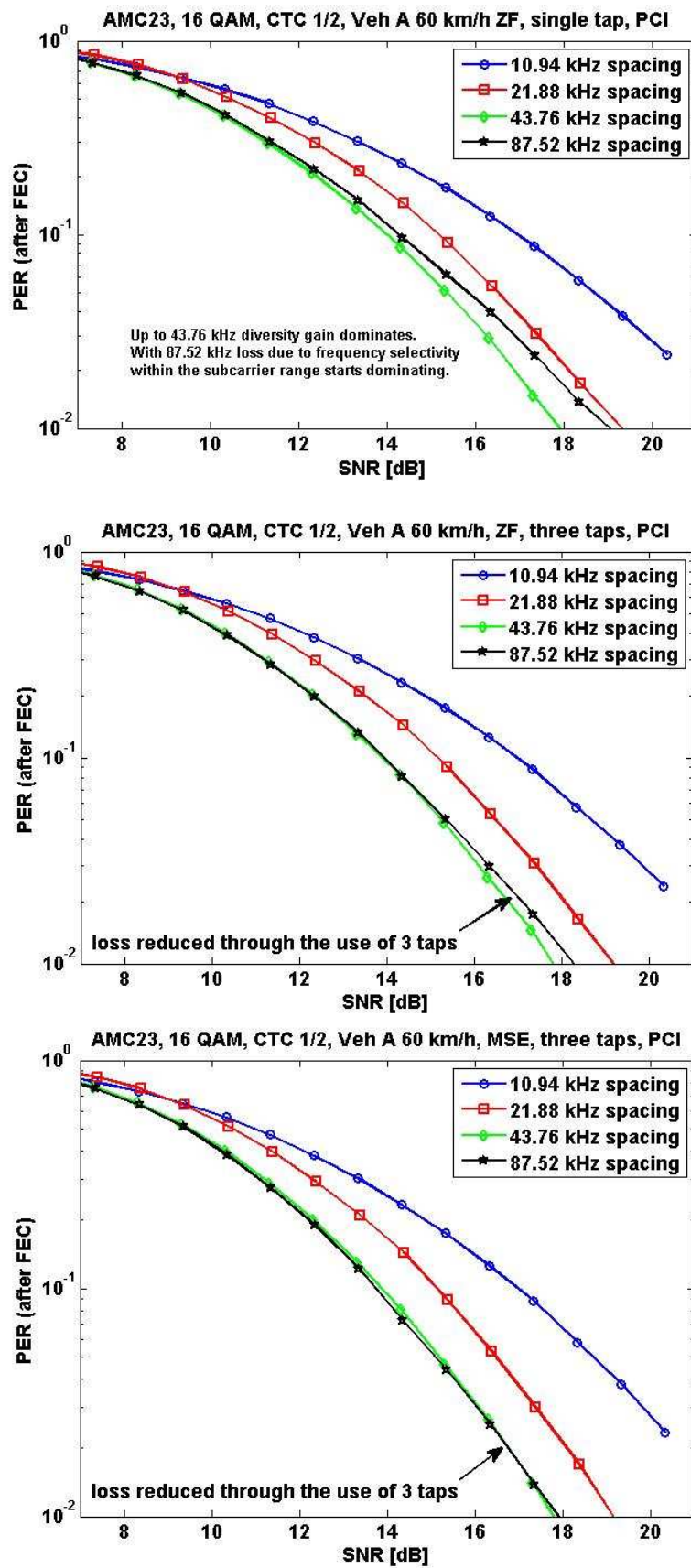


Figure 11: PER performance (after FEC) for different equalization strategies (Veh A 60 km/h)

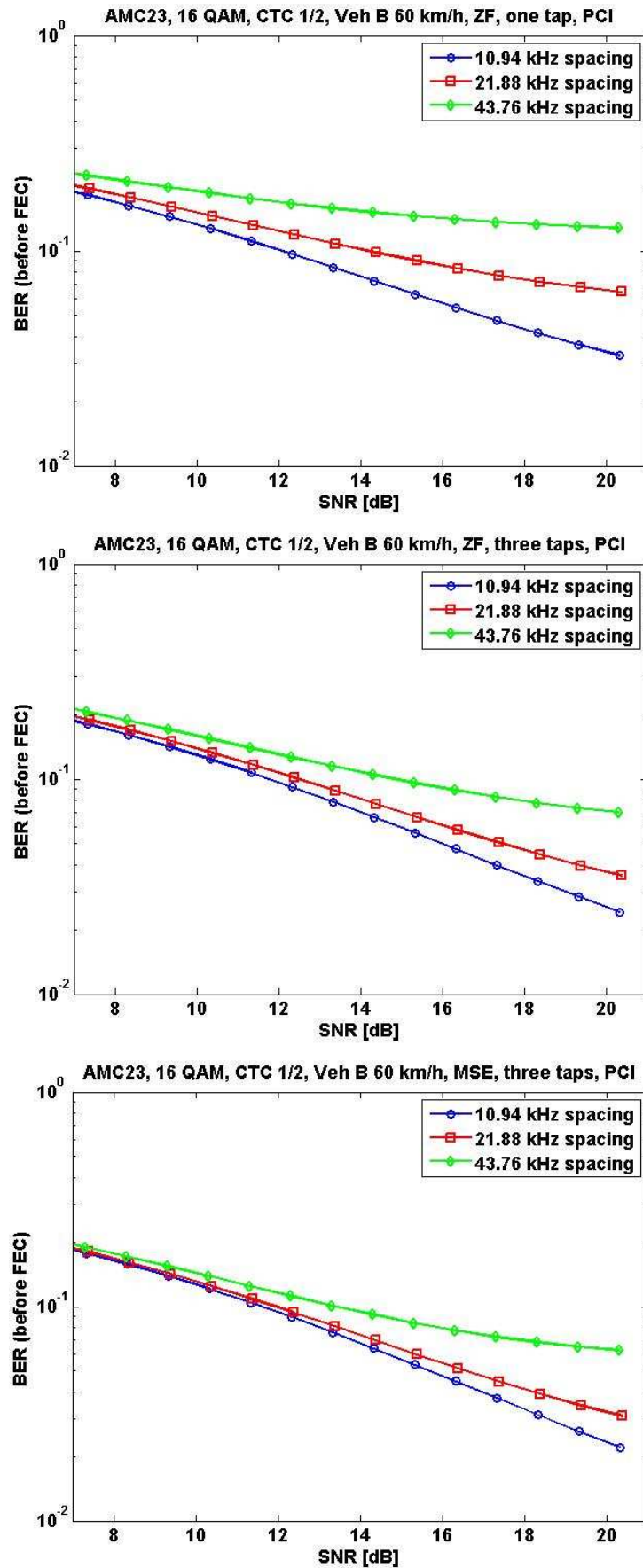


Figure 12: BER performance (before FEC) for different equalization strategies (Veh B 60 km/h)

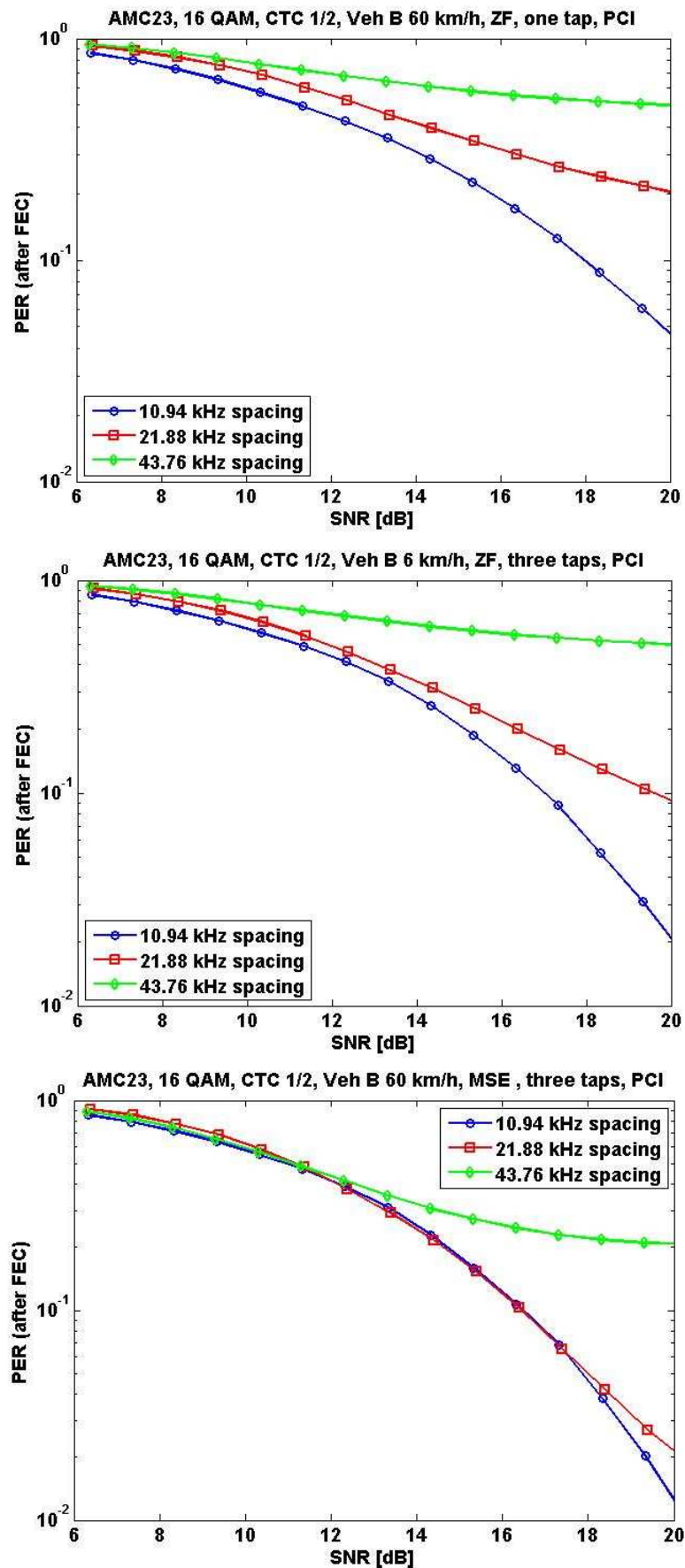


Figure 13: PER performance (after FEC) for different equalization strategies (Veh B 60 km/h)

Several impacts are visible:

- With increasing subcarrier spacings the frequency selectivity within the subcarrier range increases reducing BER performance (Figure 8 and Figure 10), if single tap equalization is used. Loss significantly reduced by using 3 taps.
- With increasing subcarrier spacings the frequency range a FEC block spans is increasing. Therefore, the diversity gain is increasing (Figure 9 and Figure 11). With 87.52 kHz the loss due to the frequency selectivity within the subcarrier range gets dominant, if single tap equalization is used. If 3 taps are used, gain due to increased diversity not totally consumed any more.
- Veh B considers much higher delay spreads than Veh A leading to a much smaller coherence bandwidth. Here, already with a spacing of 10.94 kHz the channel within the range of a single subcarrier cannot be treated as flat. Increasing the subcarrier spacing is not advisable in scenarios reflected with such high delay spreads. Once real channel estimation is applied things should even get worse. The diversity gain here naturally is smaller, as the correlation between the channel coefficients of adjacent slots is rather small even with small spacings. Even 10.94 kHz leads to significant diversity between and within the slots.
- With 10.94 kHz and 21.88 kHz (Ped B and Veh A) no gain through the use of several taps, as the channel within the subcarrier range is almost flat. With Veh B even with 10.94 kHz three taps have to be used to be able to equalize the channel.

These results nicely illustrate the fact that similar bit error rates before error correction not necessarily lead to similar performance after error correction. Obviously the bit error rate before error correction does not tell the complete story.

The used subcarrier spacing naturally impacts channel estimation based on scattered pilots. If the position of the pilots within the frame is kept, their distance in Hz grows with growing spacings. Thus interpolation accuracy between the pilots suffers.

The following figures confirm these assumptions:

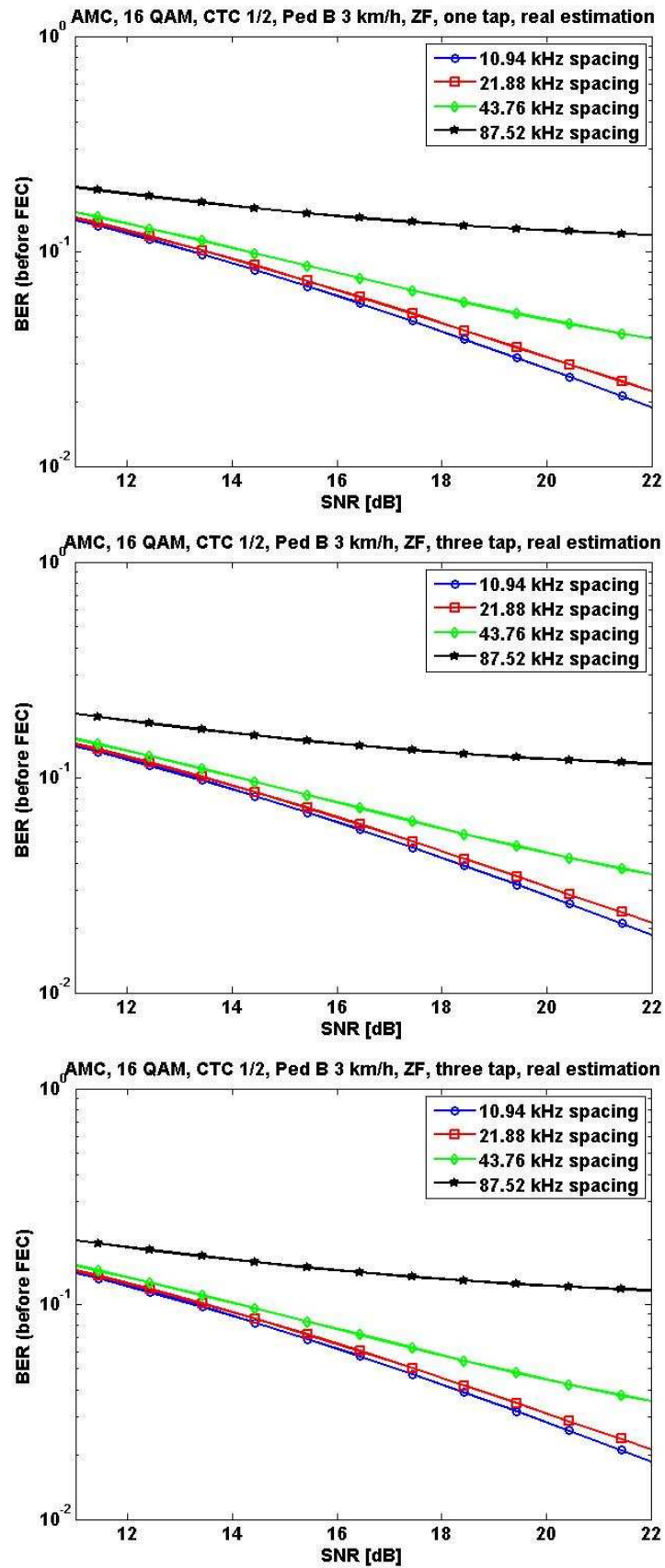


Figure 14: BER performance (before FEC) for different equalization strategies (Ped B 3 km/h) with real channel estimation based on linear interpolation

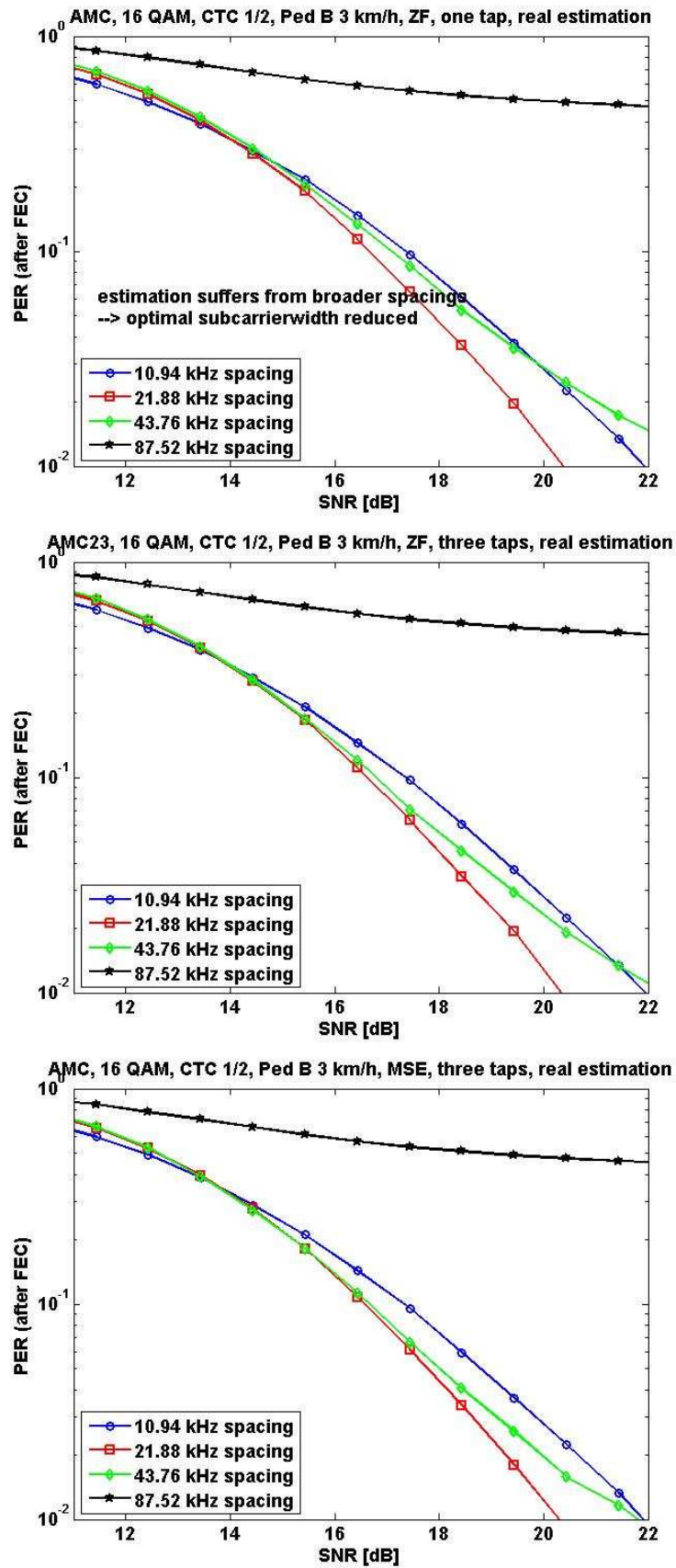


Figure 15: PER performance (after FEC) for different equalization strategies (Ped B 3 km/h) with real channel estimation based on linear interpolation

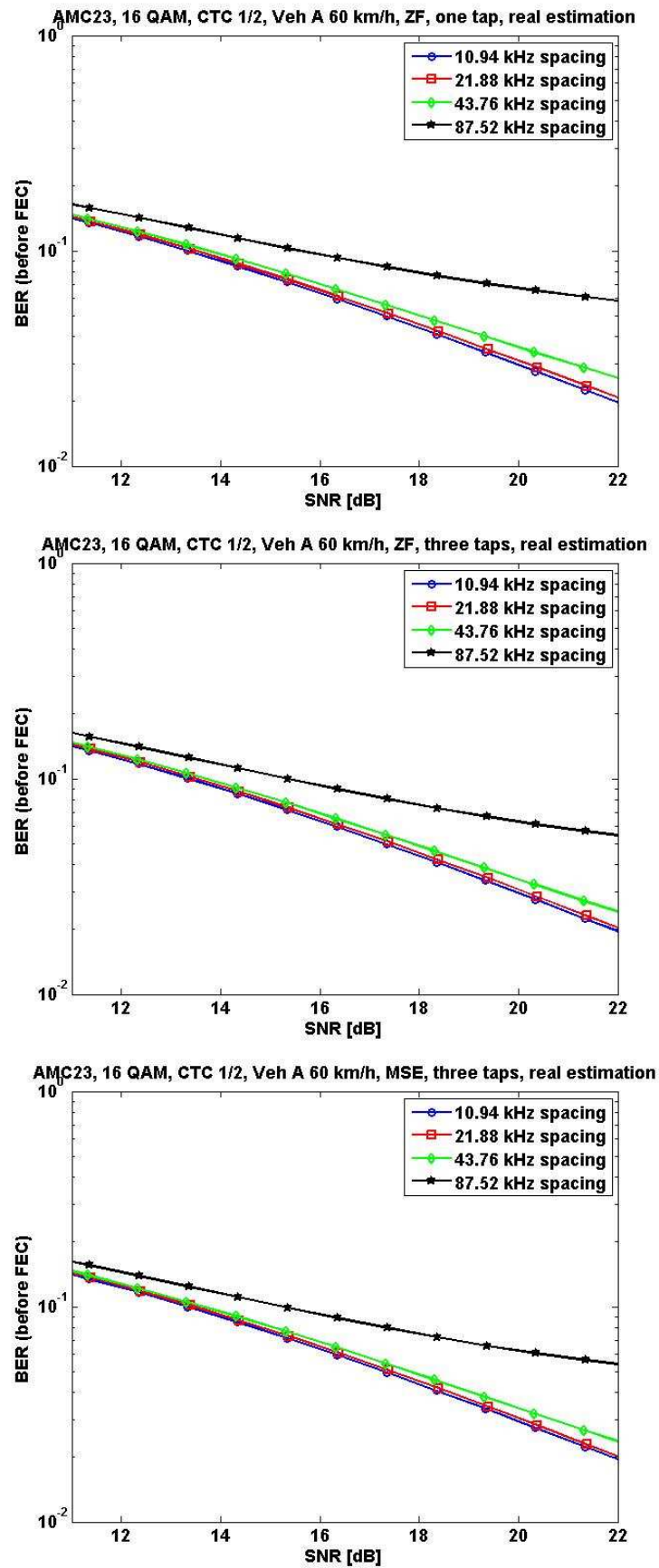


Figure 16: BER performance (before FEC) for different equalization strategies (Veh A 60 km/h) with real channel estimation based on linear interpolation

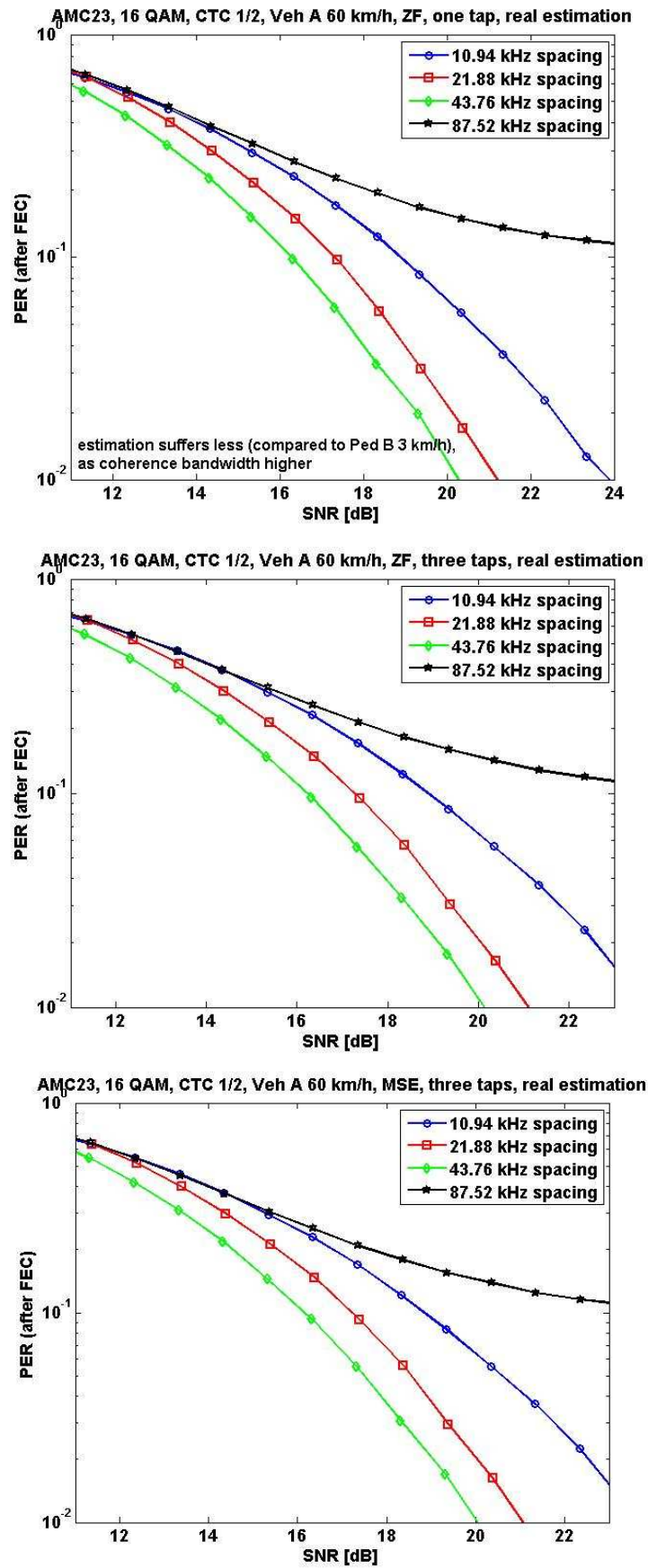


Figure 17: PER performance (after FEC) for different equalization strategies (Veh A 60 km/h) with real channel estimation based on linear interpolation

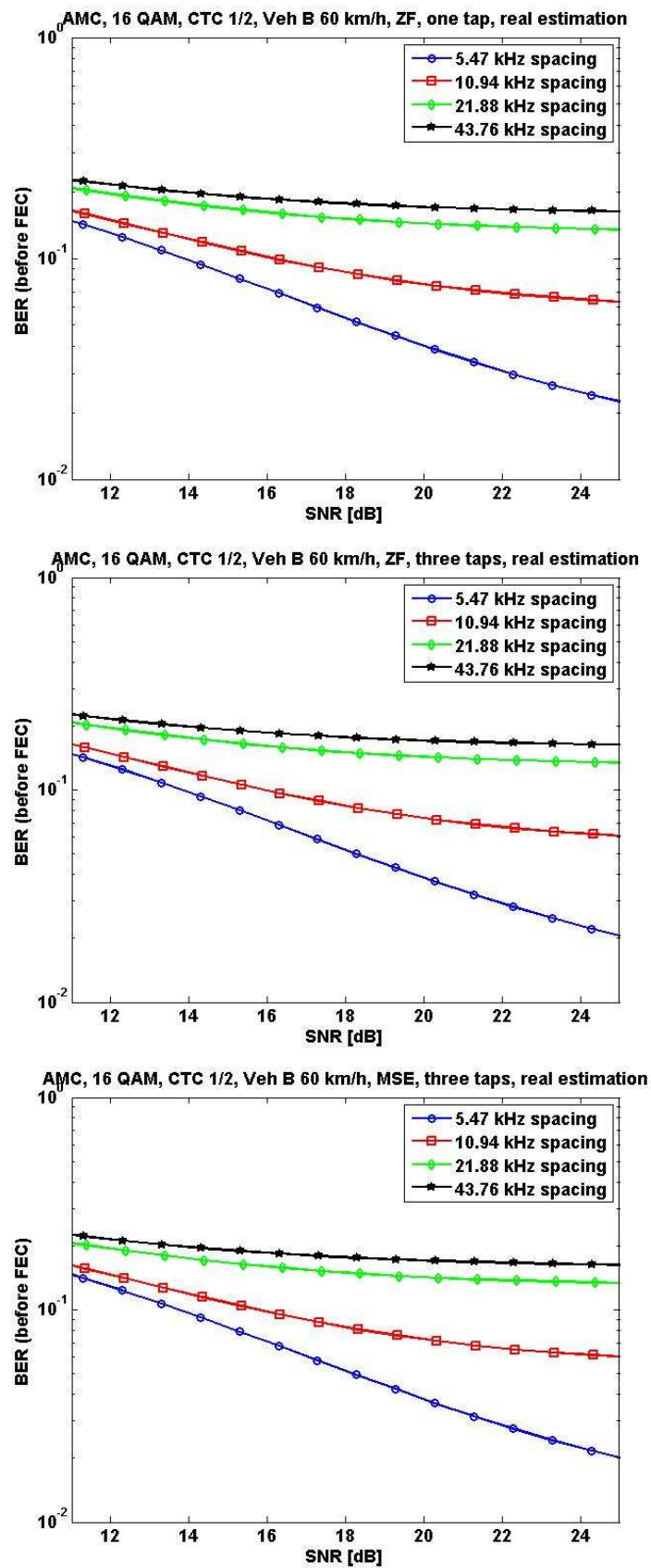


Figure 18: BER performance (before FEC) for different equalization strategies (Veh B 60 km/h) with real channel estimation based on linear interpolation

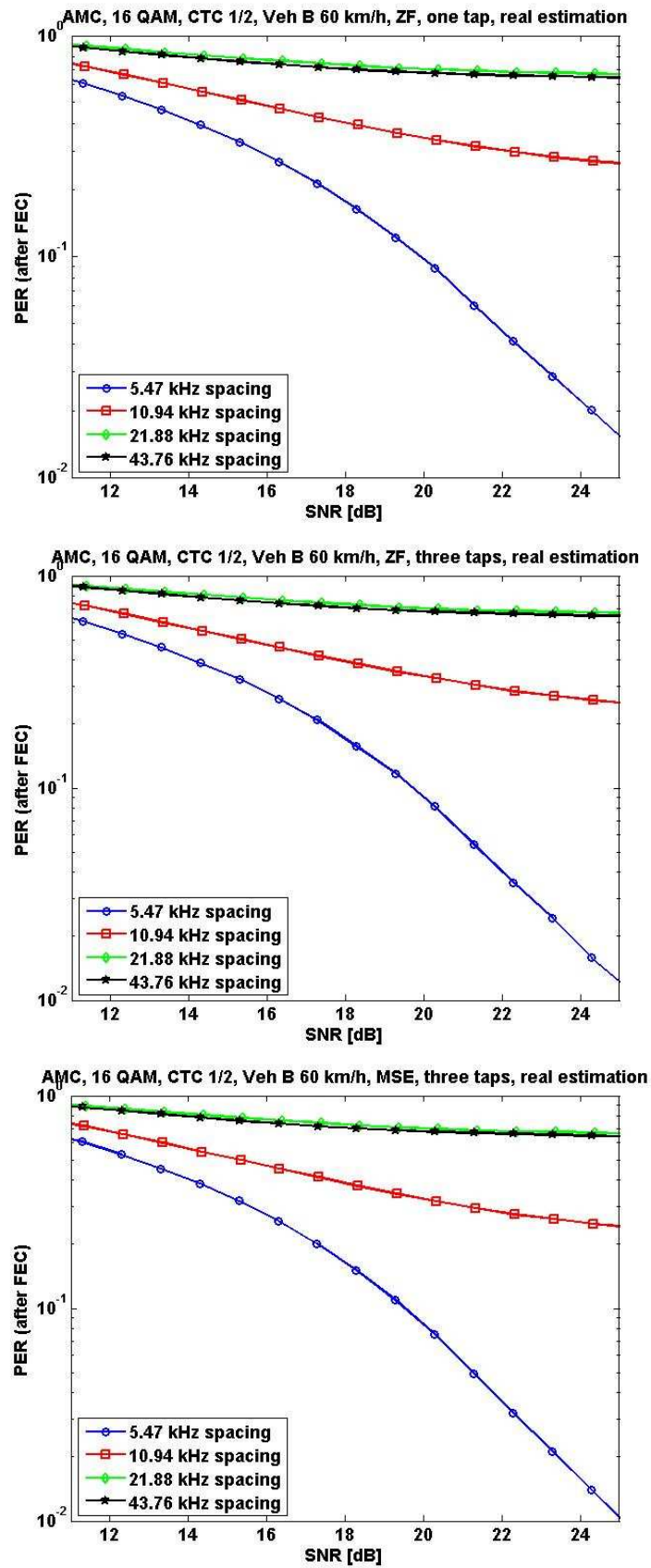


Figure 19: PER performance (after FEC) for different equalization strategies (Veh B 60 km/h) with real channel estimation based on linear interpolation

Table 4 summarizes the results. As expected the best channel spacing with respect to PER performance depends heavily on the channel characteristics (delay spread, Doppler spread).

Table 4: Optimal spacings for different channel models under the given constraint (spacing needs to be a multiple of the WiMAX spacing)

channel model	best spacing with respect to PER performance
Ped B 3 km/h	21.88 kHz
Veh A 60 km/h	43.76 kHz
Veh B 60 km/h	< 5.47 kHz

Increasing pilot density in frequency direction while decreasing pilot density in time direction (to keep overall pilot overhead constant) could improve channel estimation. A possible pilot scheme is depicted in Figure 20:

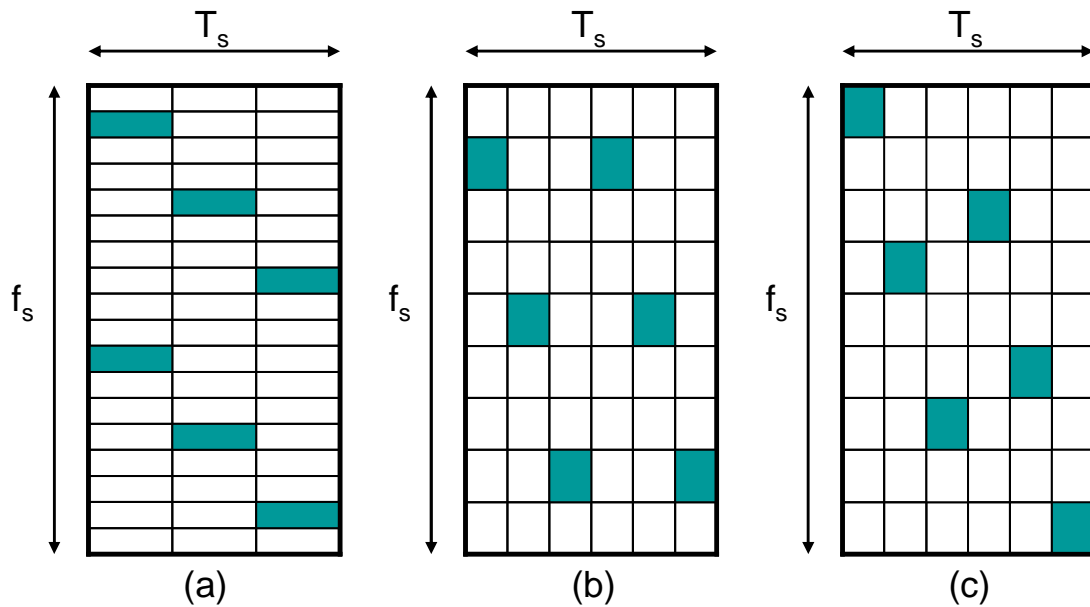


Figure 20: (a) WiMAX placement, 10.94 kHz; (b) WiMAX placement, 21.88 kHz; (c) alternative placement 21.88 kHz (white rectangle = data, blue rectangle = pilot)

Figure 20 (a) depicts the pilot placement as it is done in WiMAX in the case of AMC (f_s = frequency range of a single subchannel with WiMAX spacing, T_s = time range of a single time slot with WiMAX symbol lengths). In time direction pilots occur periodically every T_s seconds. The minimal distance between the pilots in frequency direction is 32.82 kHz. If this scheme is kept in the case of broader spacings (Figure 20 (b)) the frequency distance is increasing (e.g. 21.88 kHz spacing \rightarrow 65.64 kHz minimal distance between pilots) while the period in time direction is halved. Figure 20 (c) finally depicts an exemplary alternative pilot placement, where the average frequency distance again is lower. Here tolerance to high delay spreads/low coherence bandwidths is increased, if the coherence time exceeds T_s . On the other side the estimation of carrier frequency offsets gets penalized. The optimal scheme naturally depends on the targets of the system. If higher speeds of the mobiles are to be supported, pilot distance in time direction must be lowered; if higher delay spreads are to be tolerated pilot distance in frequency direction must not be too high.

Conclusion:

The capability of the forward error coding (FEC) scheme to benefit from frequency diversity increases with increased spacings (naturally not infinitely), as the FEC blocks are spread over a broader frequency range. This way the probability of an error burst, the FEC cannot handle, is significantly reduced.

Obviously, if the characteristics of the cells are in that way, that the delay spreads are within the range as in Ped B and Veh A, broader spacings easily can be supported. This way for a given bandwidth the number of subcarriers is reduced leading to an overall reduction of the system complexity (holding for both the filterbanks and the synchronization/equalization subsystems) in number of multiplications per multi carrier symbol. Naturally the number of multiplications per second is not affected in that way, as the duration of the multi carrier symbols is reduced when the spacing is increased. The need of chip area is traded for the necessary speed of the circuits.

4 Compatibility at initialization

High performance transmission systems require an initialization phase which, generally, consists of time and frequency alignment, as well as channel measurement to provide the information needed for equalization. In OFDM systems, this task is carried out by the FFT, exploiting a preamble and specific signals called pilots.

FBMC systems also include an FFT, which can be disconnected from the PPN (polyphase network) during initialization. Then, FBMC systems can use the same schemes and the same preamble and pilot signals as OFDM.

However, it is important to optimize both the initialization phase and the transition phase before data transmission. To this purpose, an efficient approach, which is easy to implement and provides a smooth transition to the FBMC data transmission phase, is the memory preloading technique. The technique has been presented in document D2.1 [14], it is recalled here for the sake of completion.

4.1 The memory preloading technique

The FBMC technique exploits a bank of filters derived from a prototype filter through uniform frequency shifts. As far as initialization is concerned, the issue with the approach is the impulse response of the prototype filter which imposes a transition phase. An illustration is given in Figure 21, where the system has 128 sub-channels and the synthesis filter bank (SFB) in the transmitter generates a real signal, which implies that 256 sub-channels are used altogether, to account for both positive and negative frequencies. The prototype filter length is $L=1025$ and the symbol overlapping factor is $K=4$. The impulse response of the prototype filter shown in Figure 21 provides the coefficients of the filter bank.

A crucial feature for the initialization issue is that the frequency response of the prototype filter is zero at the frequencies which are integer multiples of the sub-channel spacing, as shown in Figure 22. With this feature, at their centre frequencies, the filters in the bank are independent.

The delay of the linear phase prototype filter is $(L-1)/2=512$, which corresponds to 2 multicarrier symbols. When data are applied to the system, a transition phase of 2 symbols is introduced, as illustrated in Figure 23.

Now, the objective is to show how the prototype filter transition phase for the preamble can be skipped, which will lead to the same situation as OFDM.

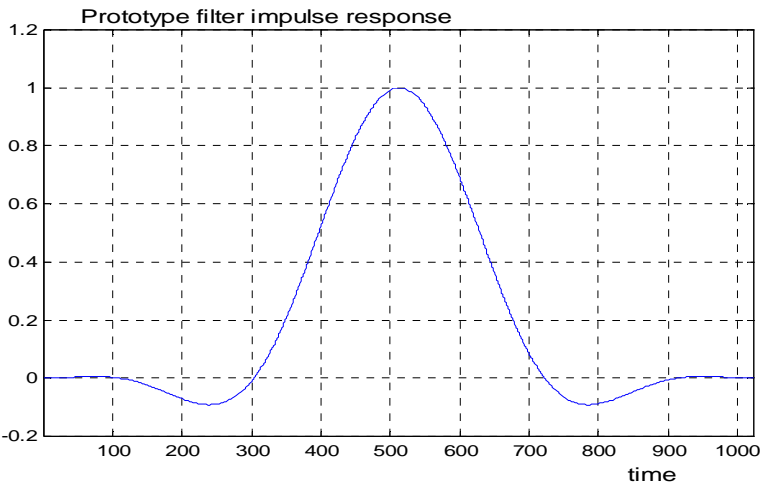


Figure 21: An example of prototype filter impulse response

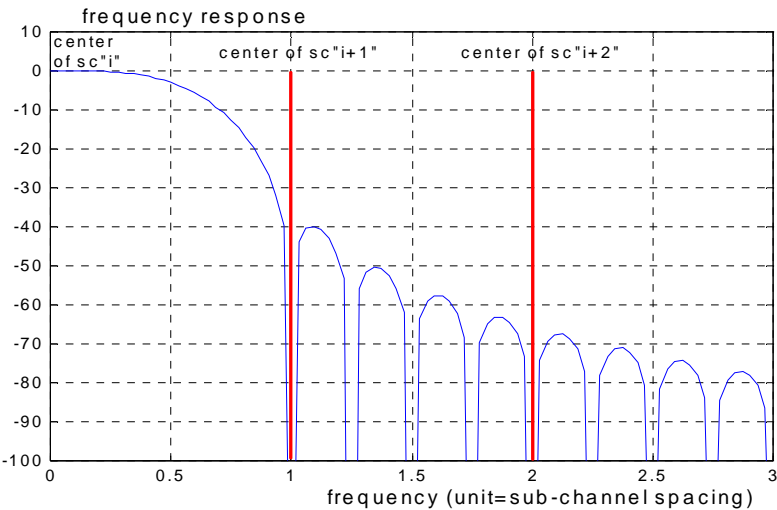


Figure 22: Frequency response of the prototype filter and positioning of adjacent sub-channels

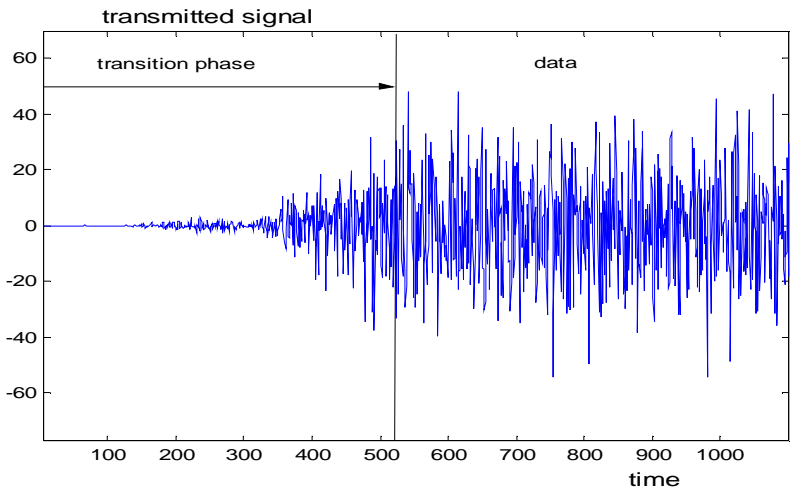


Figure 23: Transition phase in the transmitted signal

In an FBMC system, the synthesis filter bank (SFB) of the transmitter consists of the inverse FFT and the polyphase network (PPN), as shown in Figure 24. The iFFT receives the set of data to be transmitted at each symbol and its output is propagated in the memories of the PPN at the symbol rate. The SFB output, $y(n)$, is fed to the channel.

Now, if the same set of data is repeated at the input of the synthesis filter bank, the same set of samples appears repeatedly at the output of the inverse FFT and it is stored in the memories of the polyphase network. Then, all the memories of the polyphase network contain the same set of samples. In these conditions, a periodic signal is generated by the SFB and fed to the channel. At the output of the channel, the received signal is periodic and the period is the multicarrier symbol duration. The structure of the analysis filter bank (AFB) in the receiver is shown in Figure 25. The received signal $r(n)$ is fed to the memories of the PPN, which contain the same set of samples each. From the content of these memories, the receiver restores the transmitted data.

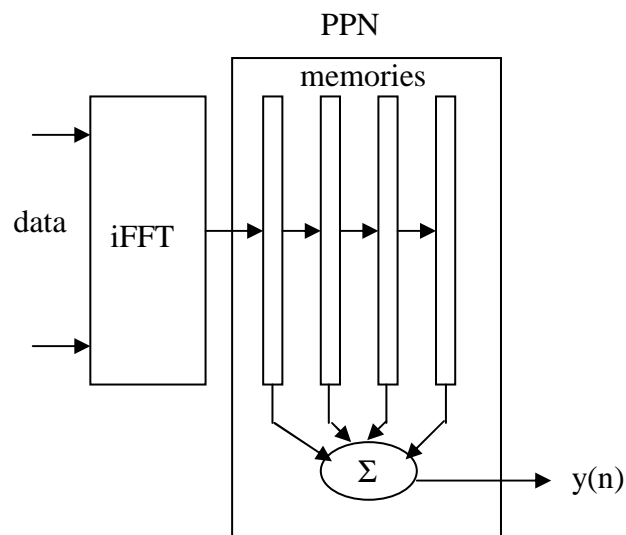


Figure 24: Structure of the SFB in the transmitter

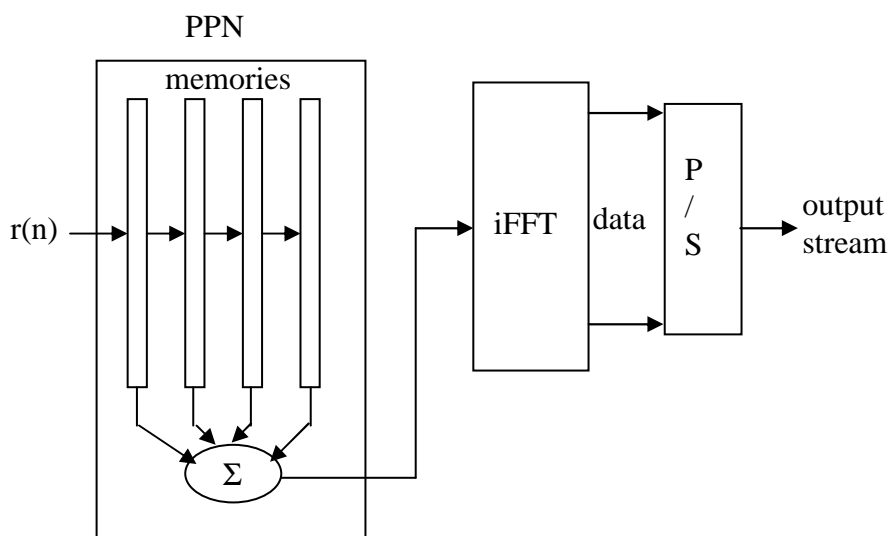


Figure 25: Structure of the AFB in the receiver

Now, if a periodic signal $y(n)$ is to be generated without any transition phase, it is sufficient to preload the memories of the synthesis filter bank with the set of samples produced by the inverse FFT. Then, to demodulate the signal at the output of the channel without the transition phase, it is sufficient to fill the AFB memories with the first received set of samples corresponding to the symbol length. With this preloading technique, implemented in both the transmitter and the receiver, there is no transition phase for the preamble. In fact, in the filter banks, the PPN has been neutralized, only the FFT remains, as in OFDM.

As concerns the data, they are not periodic and the transition phase must be kept if the highest level of performance is required. Therefore, the transition between initialization and data transmission must be investigated, to have a complete view of the OFDM-FBMC compatibility issue.

4.2 Cascading preamble and data in OQAM modulation

When maximum efficiency is sought, the FBMC approach resorts to OQAM modulation, in which the multicarrier symbol rate is the inverse of the sub-channel frequency spacing as in OFDM, but the equivalent of the real and imaginary parts of the complex data are shifted in time by half a symbol duration. The two interleaved sequences obtained are added to form the transmitted signal. In the preamble, there is little to be gained with the interleaved sequence and it is set to zero, which is the equivalent of the BPSK modulation in OFDM.

The preamble symbols and the data symbols appearing in the two interleaved sequences are shown in Figure 26, where the preamble symbols are denoted by P and the data symbols are denoted by D_i and D'_i .

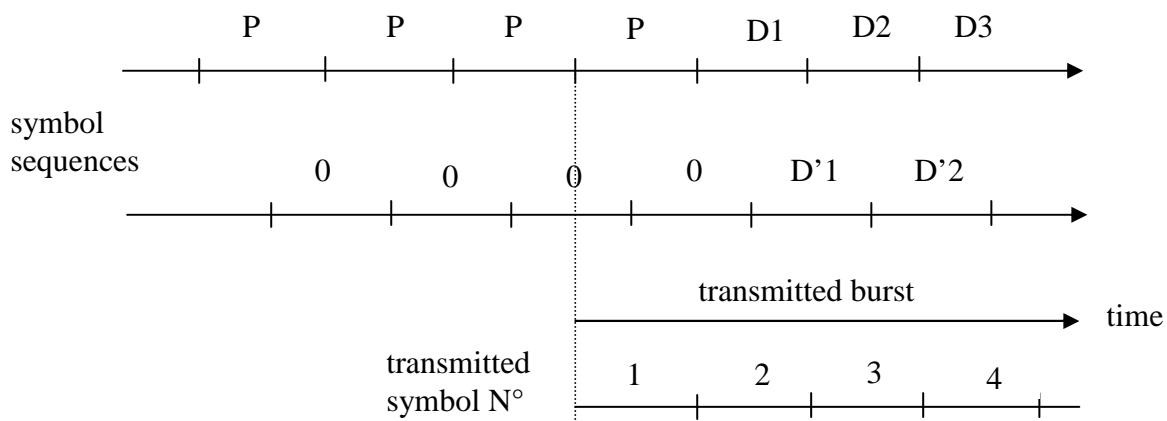


Figure 26: Symbol sequences and transmitted burst

According to the memory preloading technique, the latest time for the transmitted burst to start is the last preamble symbol, as shown in the figure. With this scheme, the first M transmitted samples, M being the number of samples in the duration of a multicarrier symbol, contain the preamble symbol P only. The contributions of the preamble and data symbols in the 4 first transmitted sets of M samples are shown in Figure 27.

Next, the first received M samples are loaded into the memories of the AFB of the receiver to demodulate the first preamble symbol. The demodulation of the first data symbol $D1$ takes place when the K memories of the receiver AFB contain the symbol $D1$, i.e. 4 symbols after. The 3 demodulated symbols in-between are preamble symbols.

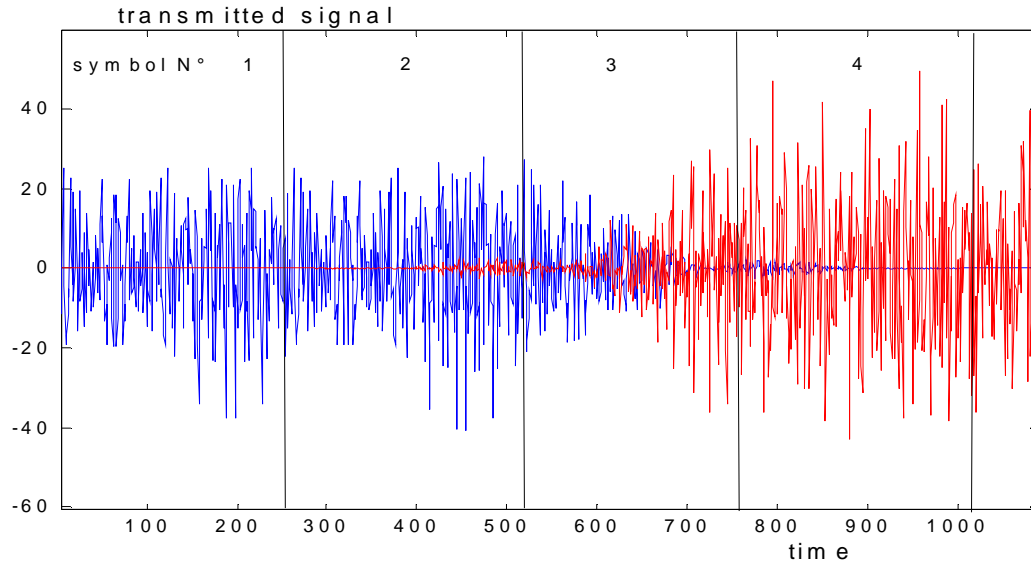


Figure 27: First transmitted sets of M samples (blue : preamble ; red : data)

An illustration is given in Figure 28. In the simulation, the filter bank parameters are as indicated in the above sections, 115 sub-channels out of 128 are used and the corresponding samples at the output of the AFB are serialized, as shown in Figure 25, to provide the output data stream and give a global view of the transmission channel. Note that half the transmission capacity is used in the preamble, since the interleaved sequence has been set to zero as indicated at the beginning of next section.

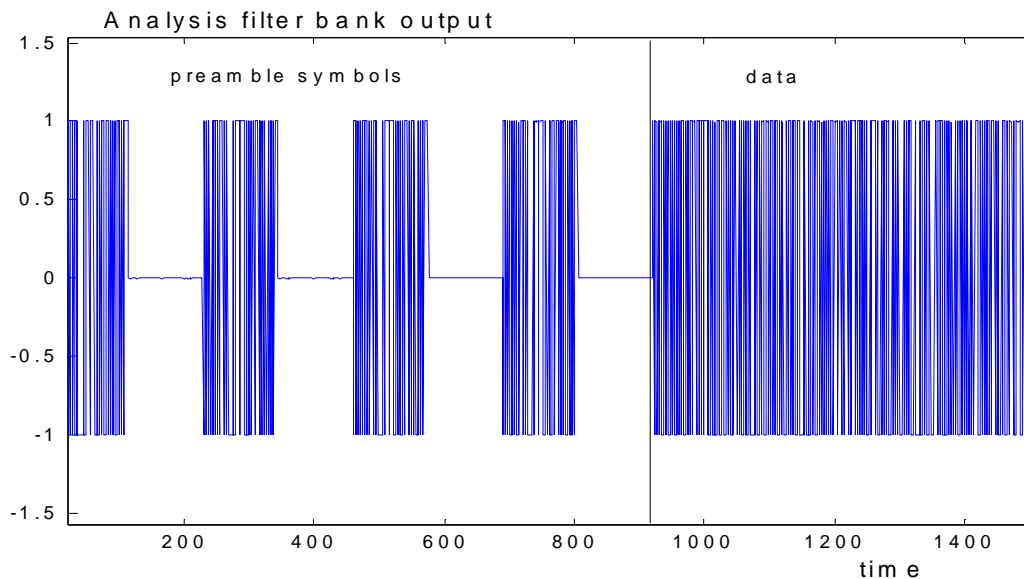


Figure 28: Output of the AFB in the receiver after serialization

In this simulation, the SFB and AFB are connected back to back, no transmission channel is present.

Next, some estimation techniques, which are commonly used in OFDM systems, are reviewed in the FBMC context.

4.3 Transmission parameter estimation

As attested by Figure 21, Figure 22, Figure 23 and Figure 27 above, the first half of the second set of M transmitted samples contains a very small contribution of the data symbol $D1$ and, therefore, it can be considered as a repetition of the preamble symbol, which is necessary to estimate the channel parameters.

To begin with, the carrier frequency offset can be measured by conventional techniques, based on the signal repetition mentioned above.

Next, the frequency response of the channel is given by the output of the receiver AFB. An illustration is given by simulation. A channel with deep fading and the impulse response shown in Fig.8 is inserted between the transmitter and the receiver.

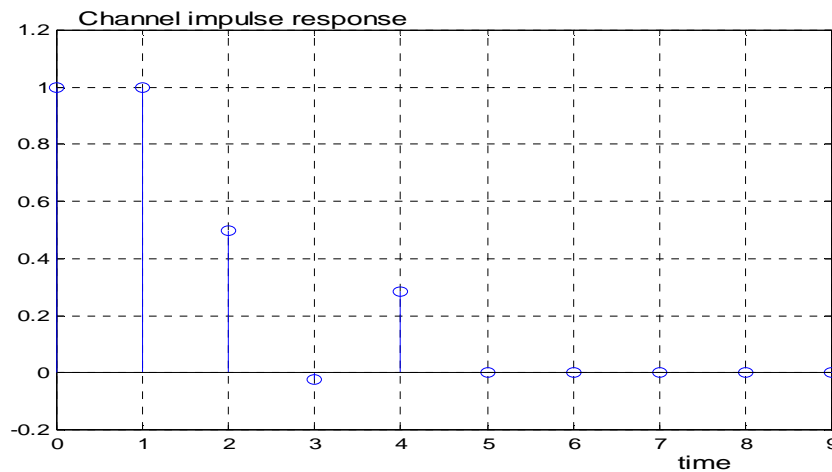


Figure 29: Channel impulse response

The discrete Fourier transform of this impulse response is used to equalize the sub-channels at the output of the AFB in the receiver. The signal obtained after serialization is shown in

Figure 30.

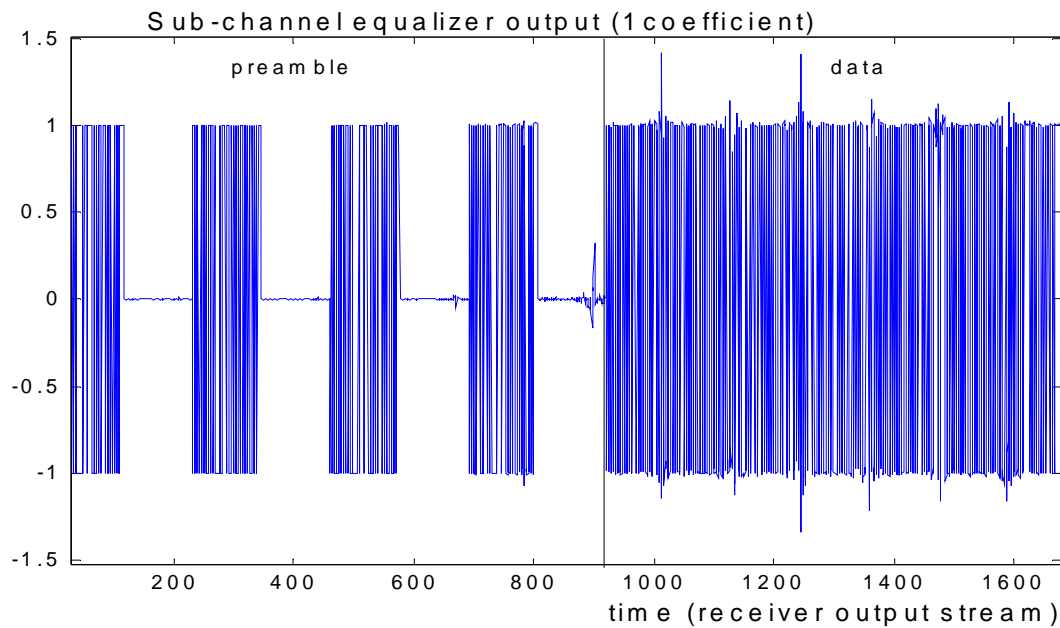


Figure 30: Output of the AFB after equalization and serialization

In the first preamble symbol, since there is no superposition of preamble and data signals, the AFB output is perfectly equalized by the FFT of the channel, which means that the filter bank approach and the FFT lead to the same estimation.

The next step is the determination of the timing offset in the receiver, using the outputs of the sub-channels. A simple and efficient technique consists of eliminating the modulation at the output of each sub-channel and, then, computing the inverse FFT, which provides an estimation of the channel impulse response. For example, a delay of 10 samples is introduced at the receiver input and the channel impulse response estimated in this manner is shown in Figure 31. The delay is correctly estimated.

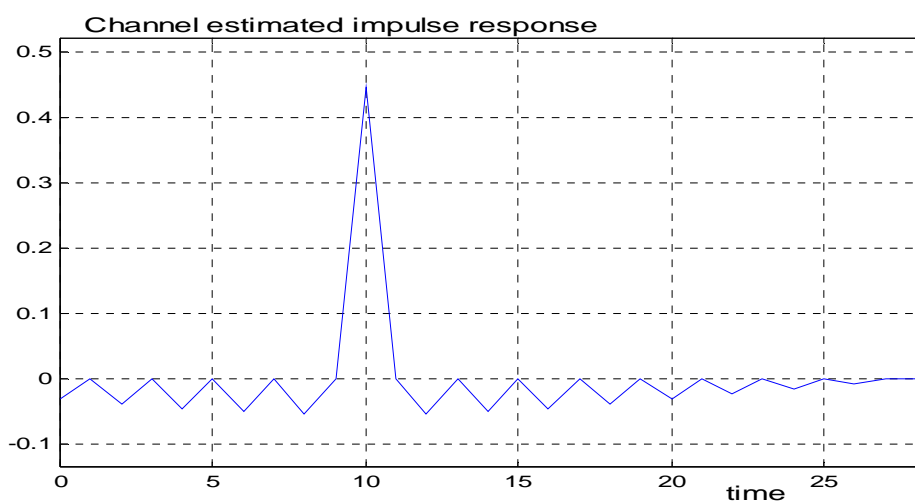


Figure 31: Channel impulse response estimation, in the case of a pure delay

Now, the channel impulse response of Figure 29 is combined with the delay of 10 samples. The estimated impulse response is shown in Figure 32. Again, the delay is correctly estimated.

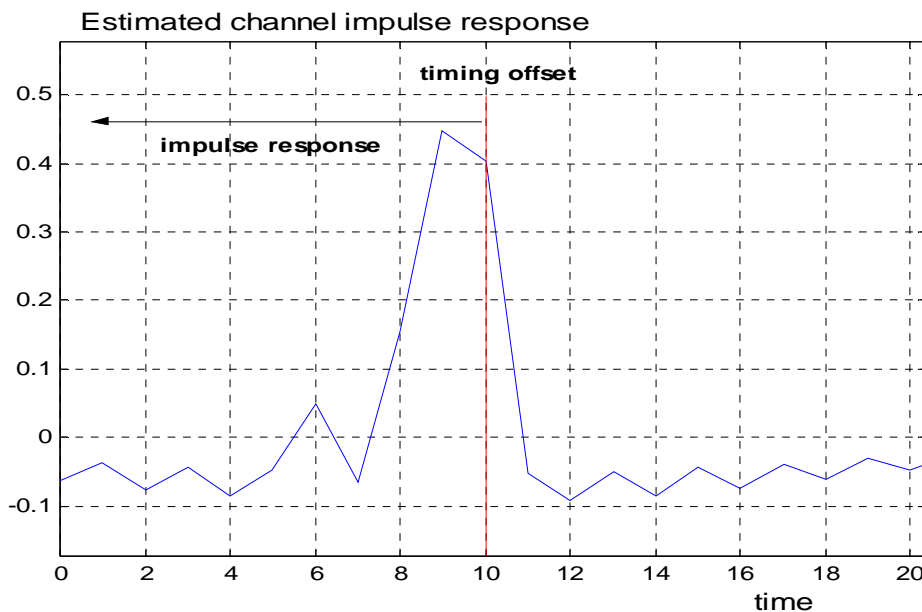


Figure 32: Estimation of time offset in the presence of channel distortion.

Then, the robustness to additive white Gaussian noise is investigated. The availability of several preamble symbols in the receiver can be exploited to carry out noise measurements and improve the signal to noise ratio.

The presence of 4 preamble symbols in the receiver is due to the fact that the symbol P is present in 4 consecutive blocks of M samples in the transmitted burst. When noise is added to the channel, the first received set of M samples contains noise samples which are preloaded in the AFB memories along with the useful signal. As a consequence, the noise samples which are added to the preamble symbols at the AFB output are correlated and the expected SNR improvement provided by averaging over 4 blocks is less than 6 dB.

An illustration is given in

Figure 33. The channel has no distortion, only additive noise and the SNR is 20 dB. The measurement of the noise power for each of the 4 preamble symbols yields the following numbers: [0.0074 0.0080 0.0064 0.0076]. After signal averaging, the noise power is 0.0035, which is a reduction of about 3 dB.

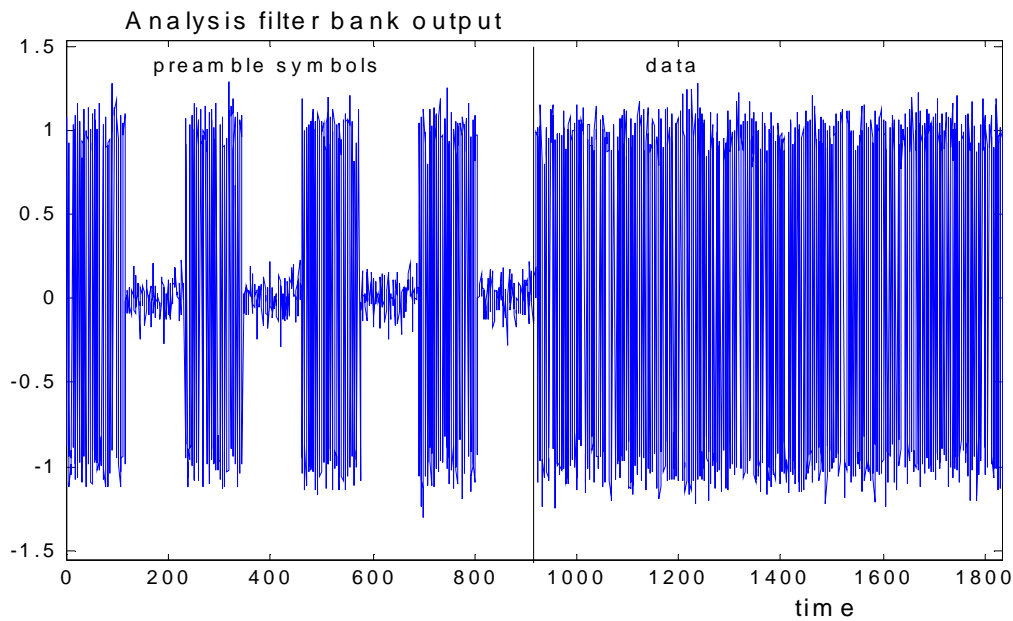


Figure 33: Output of the AFB after serialization, with SNR=100 (20 dB)

Although the transmitted signal shown in Figure 27 is specifically designed for FBMC systems to fully exploit the context, it can be exploited by an OFDM system as well, to obtain the channel parameters. By applying an FFT to the first symbol, CFO, channel frequency response and timing offset are derived as above. However, in the second and third initialization symbols, the data signal is present and it impacts the measurements.

Next, the MIMO case is considered and some OFDM techniques are applied to the FBMC context.

4.4 Memory preloading with MIMO

In MIMO systems, a receiver is connected to several transmitters and the corresponding channel responses must be estimated. The case of 2 transmitters is shown in Figure 34.

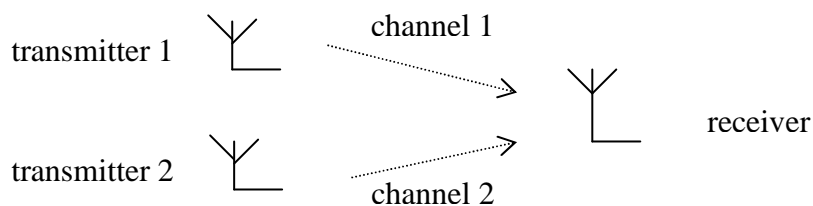


Figure 34: MIMO system (2x1)

With the memory preloading technique, it is possible to perform the measurements of two channels simultaneously, invoking the periodicity of the signals.

The frequency responses of adjacent filters in the bank are shown in Figure 35. At the centre frequency of filter « i », the responses of neighbouring filters « i-1 » and « i+1 » are null, as pointed out at the end of section 1. Therefore, in the presence of constant signals at the synthesis filter bank inputs there is no interference between the sub-channels. Then, it is possible to use the sub-channels with odd indices to estimate one of the 2 channels and the sub-channels with even indices to estimate the other channel. Finally, the channel responses at all the sub-channel centre frequencies can be obtained through interpolation.

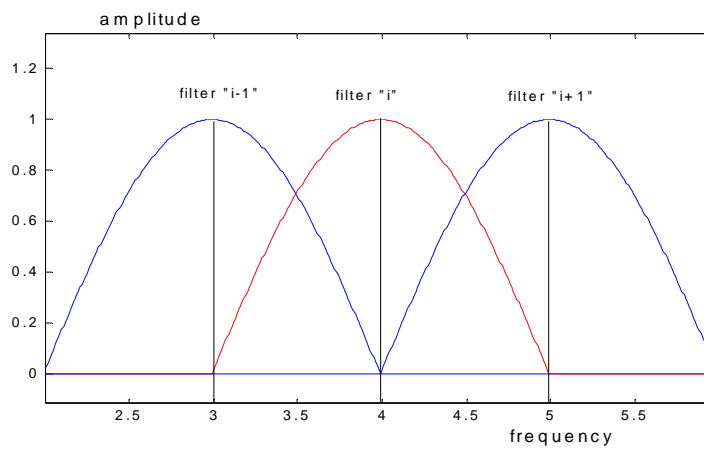


Figure 35: Frequency responses of adjacent filters within the filter bank

The process is illustrated in Figure 36. In the simulation, two different channels with deep fading are used and the coefficient vectors are

$$\begin{aligned} h_1 &= [1 \ 1 \ 0.5 \ -0.025 \ 0.285] \\ h_2 &= [1 \ -1 \ 0.5 \ 0.025 \ 0.285] \end{aligned}$$

At the output of the AFB in the receiver, single coefficient equalization is performed, using the FFT of impulse responses h_1 and h_2 for the sub-channels with odd and even indices respectively.

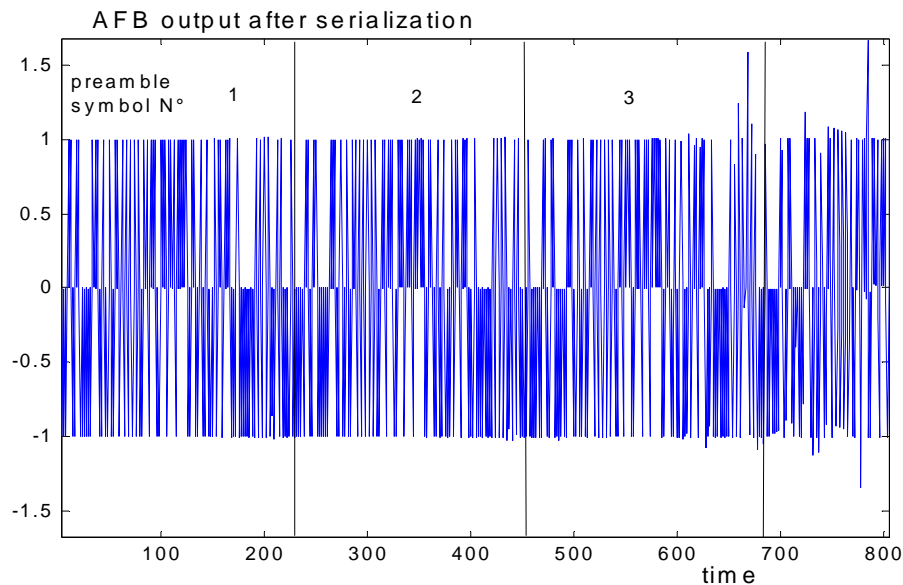


Figure 36: MIMO system (2x1) with frequency interleaved transmission

Clearly, the measurement is accurate, for the first symbol of the preamble.

The extension to MIMO systems with more transmitters can be achieved with a similar scheme. For example, in a (4x1) system, 4 interleaved groups of sub-channels can be allocated to the 4 transmitted signals. Of course, in that case, 3 frequency points have to be interpolated between two measured values.

If measurement of the channels at all the centre frequencies is required, then multiple preloading can be implemented with the corresponding increase in the duration of the initialization phase.

Note that, in a MIMO system, the transmitted signals are synchronized. The time offset and the frequency offset are the same for all the received signals.

4.5 Estimation in the cognitive radio context

A distinctive feature of the cognitive radio context is that very accurate and reliable spectrum measurements must be carried out in the presence of potentially large magnitude signals in the frequency band under analysis.

In order to illustrate the potential of filter banks, a large magnitude sine wave is introduced in the middle of the transmission band. The preloading technique is applied, with 3 preamble symbols sent before the data symbols are applied to the SFB in the emitter. The signal obtained at the output of the AFB in the receiver is shown in Figure 37. The upper sub-figure shows the real part, which is the useful signal from which the data are retrieved. The lower sub-figure shows the imaginary part, which is the interference signal. The first 6 symbols are preamble symbols, followed by data symbols.

The channel described in section 4.4 is introduced in the link and a single coefficient sub-channel equalizer is applied on each of the used AFB output. As in section 4.4, the equalizer coefficients are the inverse of the FFT of the channel impulse response, in the absence of the jammer.

The set of samples corresponding to the first symbol give a poor estimation of the channel, due to the severe perturbation caused by the large magnitude sinusoid. In fact, the situation is similar to OFDM, for which the spectral resolution of the FFT is insufficient. Then, the filter bank enters into action and, at symbol 4, accurate channel estimation is achieved, in spite of the presence of the jammer. In fact, comparing symbol 4 and symbol 1 gives a clear illustration of the superiority of FBMC over OFDM for real time spectrum sensing.

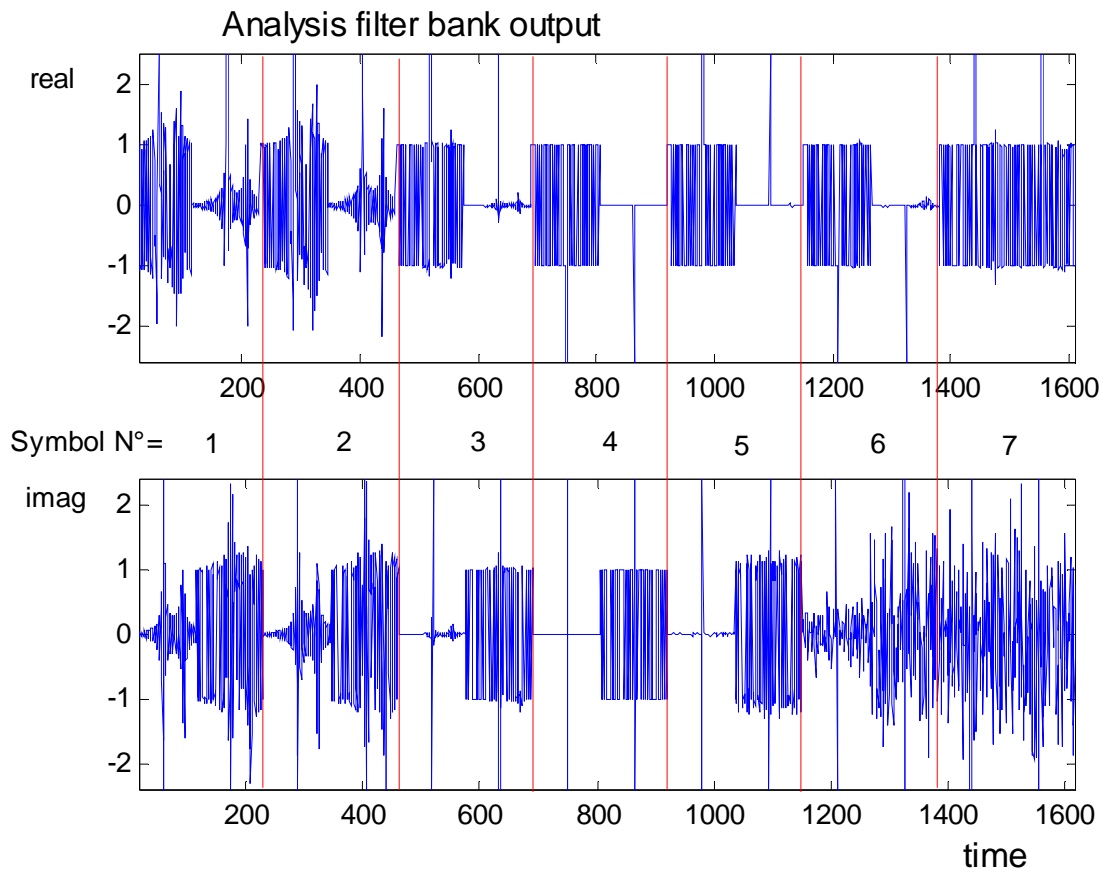


Figure 37: Analysis filterbank output in the receiver (real part and imaginary part), with a large sinusoid in the middle of the transmission frequency band.

Note that the above approach applies to channel estimation for a group of sub-channels allocated to a particular user, while others users are active, as in multiuser uplink.

4.6 Conclusion and recommendations

The filter bank memory preloading technique can be adapted to different situations:

1. The transmission starts from scratch and no channel information is available in the receiver. Then, at least one preamble symbol is applied to the transmitter input before data symbols are applied, preloading is used in transmitter and receiver, and the channel is measured at the receiver output.

2. Channel information is available at the beginning of the burst. Then, preloading can be used with the first data symbol, which is repeated K times at the output of the receiver.
3. Several channels have to be measured simultaneously for MIMO transmission. Then, the preamble symbol is distributed across interleaved groups of sub-channels and preloading is used.
4. Several channels have to be measured at all the sub-channel centre frequencies. Then, the preloading operation is repeated in both the transmitter and the receiver.
5. A high level narrow band jammer is present in the transmission channel. Then, a number of preamble symbols equal to $K-1$ is applied to the transmitter, before data symbols are applied.

5 Automatic detection of OFDM / FBMC

In this section, we propose a comprehensive OFDM (orthogonal frequency division multiplexing) modulation signal, FBMC (filter bank based multicarrier) modulation signal, and AWGN signal classification system by applying two simple detectors: preamble detector and correlation detector. A preamble existence test [16] is first applied to distinguish the desired signals with preambles from AWGN signal. When the existence of multicarrier signals is confirmed, correlation test [17] due to the inserted CP (cyclic prefix) in OFDM signal is then applied to distinguish OFDM signal and FBMC signal. The module diagram of this classification system is depicted in Figure 38.

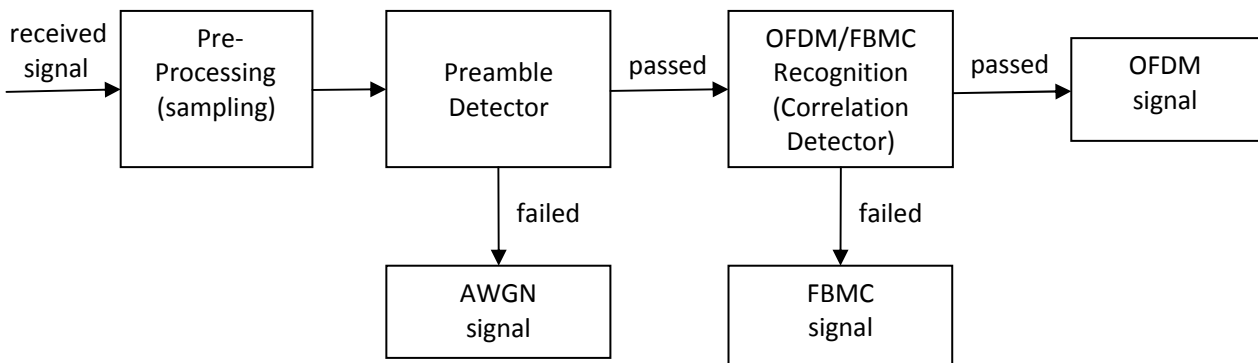


Figure 38: OFDM / FBMC / AWGN signal classification system module diagram by applying preamble detector and correlation detector.

Firstly, the received signal is processed by down-conversion and sampling, and then preamble detection and correlation detection are subsequently implemented.

1) Preamble detection

We assume that FBMC signal and OFDM signal have the same preamble structure, and the receiver end knows the preamble information. Therefore, the existence of multicarrier signals can be determined using a preamble test. If the test failed the received signal is assumed to be an AWGN signal. Otherwise, a passed test indicates that the signal is a multicarrier signal (OFDM or FBMC) and a conventional correlation detector would be applied for further processing.

2) Correlation detection

Once the multicarrier signal is confirmed, then a classic correlation detector can be used for distinguishing OFDM signal and FBMC signal. In OFDM systems, the last “ $CP * T_u$ ” (T_u is the useful period of one OFDM symbol and CP is the ratio of cyclic prefix period to useful period) of the useful symbol is copied to the front of the symbol to eliminate ISI (Inter Symbol Interference) as shown in Figure 39.

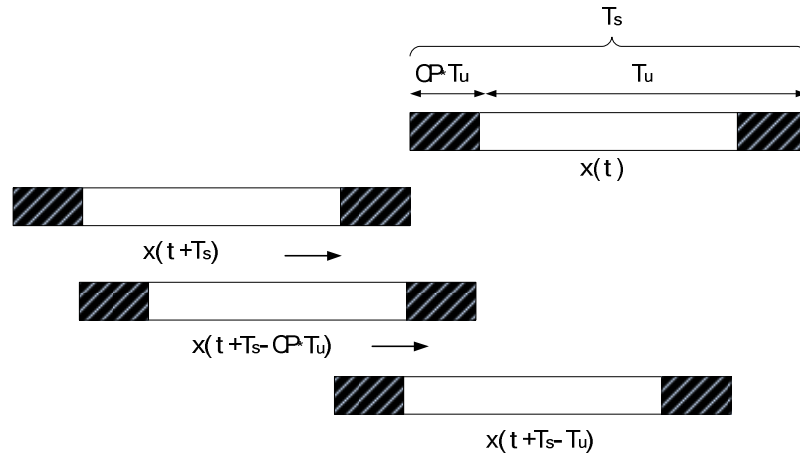


Figure 39: Correlation detection process

The principle of the correlation test is the classic autocorrelation

$$R(\tau) = \int_0^{\tau} x(t + T_s - \tau) x^*(t) dt, \quad 0 < \tau < T_u \quad (1)$$

where $x(t)$ is one OFDM symbol, and “ $T_s = CP * T_u + T_u$ ” is the full OFDM period. Figure 39 illustrates the detection process.

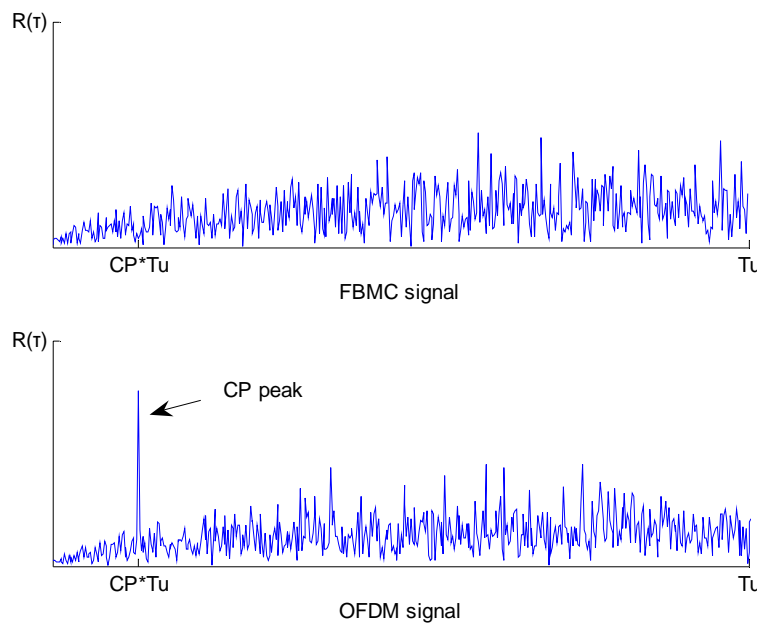


Figure 40: Correlation test of one signal symbol with $CP = 1/8$ and $SNR = 6$ dB.

Figure 40 shows the correlation test for FBMC and OFDM with one signal symbol, we can observe that a CP peak (local maximum value) appears for OFDM signal. Practically, the CP peak may be

buried resulting from noise and multipath fading, in this case, multiple signal symbols are used, and (1) is calculated individually for each symbol, then their corresponding autocorrelation results are added together so that the CP peak can be strengthened.

3) Simulation results

In order to evaluate the performance of correlation detection, we have simulated a 512-subcarriers OFDM and FBMC signal with assumed conditions as follows:

- ✓ Multicarrier signals are transmitted at the frequency band with a bandwidth of 10MHz and centre frequency 2.4GHz .
- ✓ We consider the AWGN channel and frequency selective channel, respectively. A typical urban channel is used with total twenty-two taps and spread delay " $\tau \approx 2\mu\text{s}$ ":

$\text{Delays} = 1e-6 * [0.217 \ 0.512 \ 0.514 \ 0.517 \ 0.674 \ 0.882 \ 1.230 \ 1.287 \ 1.311 \ 1.349 \ 1.533 \ 1.535 \ 1.622 \ 1.818 \ 1.836 \ 1.884 \ 1.943 \ 2.048 \ 2.140] \text{s}$;

$\text{Powers} = [-5.7 \ -7.6 \ -10.1 \ -10.2 \ -10.2 \ -11.5 \ -13.4 \ -16.3 \ -16.9 \ -17.1 \ -17.4 \ -19.0 \ -19.0 \ -19.8 \ -21.5 \ -21.6 \ -22.1 \ -22.6 \ -23.5 \ -24.3] \text{dB}$;

- ✓ The PHYDYAS reference filter bank with an overlapping factor "4" is used [18].

Our purpose is to find whether the received signal is an OFDM signal or a FBMC signal. This is a binary signal detection problem, which can be modelled as a hypothesis testing problem. There are two possible hypotheses, H_0 and H_1 :

$$\begin{aligned} H_0: \quad \mathbf{x}(t) &= \mathbf{s}_{\text{fbmc}}(t) + \mathbf{n}(t) && \text{(FBMC signal present)} \\ H_1: \quad \mathbf{x}(t) &= \mathbf{s}_{\text{ofdm}}(t) + \mathbf{n}(t) && \text{(OFDM signal present)} \end{aligned} \quad (2)$$

The probability of false alarm Q_f for a given threshold V_T is given by:

$$Q_f = P_{\text{rob}}\{V > V_T | H_0\} \quad (3)$$

For the same threshold level, the probability of detection Q_d is given by:

$$Q_d = P_{\text{rob}}\{V > V_T | H_1\} \quad (4)$$

Since the receiver knows the system parameters, such as the symbol period, cyclic prefix period, etc, cyclostationarity detector [19][20] which is generally used for blind cognitive radio signal detection is not chosen for our OFDM/FBMC detection. Herein the above correlation detection method is applied, so " $V = R(\text{CP} * T_u)$ " (see Figure 40). 1000 independent cases for H_0 and H_1 are simulated, respectively, and the false alarm probability and detection probability are computed according to (3) and (4) by choosing various thresholds V_T .

The receiver operating characteristic (ROC) curves are drawn in Figure 41 and Figure 42 for AWGN channel and Multipath channel with one signal symbol " $N = 1$ " and " $\text{CP} = 1/8$ ", respectively. Although the results deteriorate when more realistic multipath channel is considered, perfect detection performance can be achieved when using one signal symbol at the SNR levels more than 2dB regardless of the channel condition.

In order to further evaluate the performance of correlation detector, worse channel conditions (in cognitive radio context) with SNR levels ($\leq 0\text{dB}$) and different CP lengths are considered. ROC curves for the AWGN channel case with different CP lengths (1/4, 1/8, 1/16, 1/32) and SNR levels (-2dB, -4dB, -6dB, -8dB, -10dB) are shown in Figure 43 and Figure 44. Figure 43 demonstrates the effects of CP length at a fixed “SNR=-4dB”, it can be seen that the larger the CP length is, the better the detection performance is. In Figure 44, we observe that detection reliability can be seriously impacted by the decreased SNR level, which can be overcome by using multiple signal symbols as shown in Figure 45. As a comparison, effects of multipath channel are shown in Figure 46 at different signal symbol number and CP length, which indicates that the multipath channels affect detection performance especially for the case with small CP length. Figure 47 gives the detection performance with “CP=1/32” and “SNR=-4dB” at different signal symbols. Unfortunately, more signal symbols are needed to achieve the satisfactory performance in this case because the number of channel taps overpasses the number of CP length.

Simulations show that, in practice, using the correlation detector reliable detection performances can be achieved with only one signal symbol. Moreover, this correlation detector has also been evaluated in worse channel conditions (cognitive radio context) assuming the receiver knows the system parameters. However, in a cognitive radio system without prior knowledge, energy detector and cyclostationarity detector should be used instead of applying the correlation detector for blind cognitive radio signal detection.

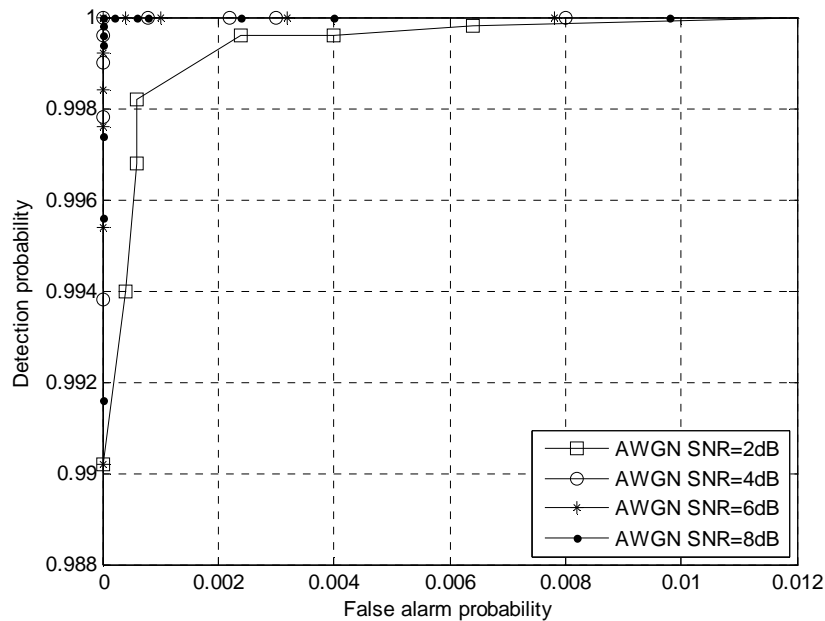


Figure 41: Receiver Operating Characteristic performance of AWGN channel for different SNR values with fixed $N = 1$ and $CP = 1/8$.

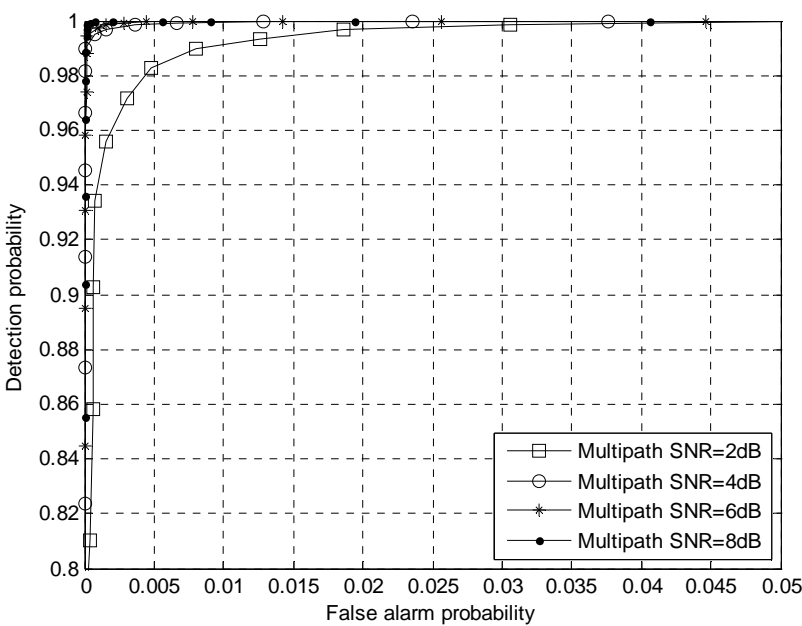


Figure 42: Receiver Operating Characteristic performance of multipath channel for different SNR values with fixed $N = 1$ and $CP = 1/8$.

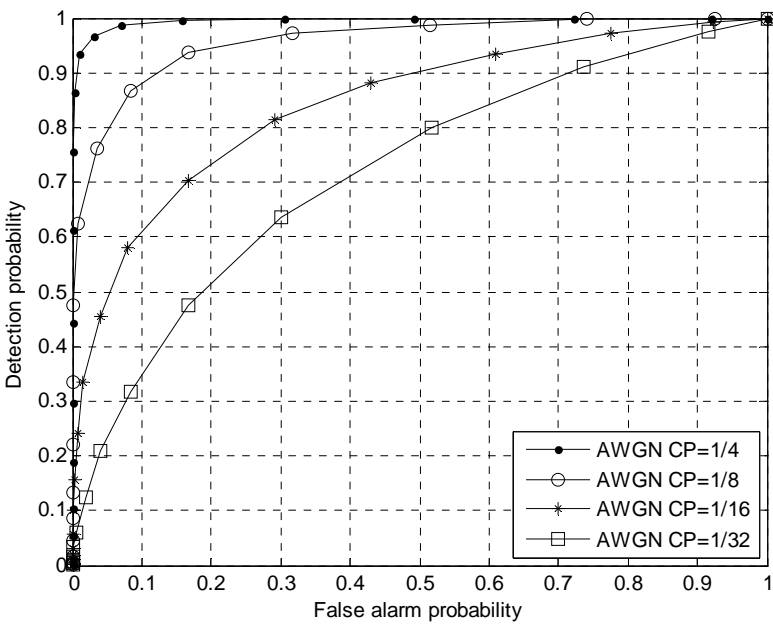


Figure 43: Receiver Operating Characteristic performance of AWGN channel for different CP values with fixed $N = 1$ and $SNR = -4$ dB.

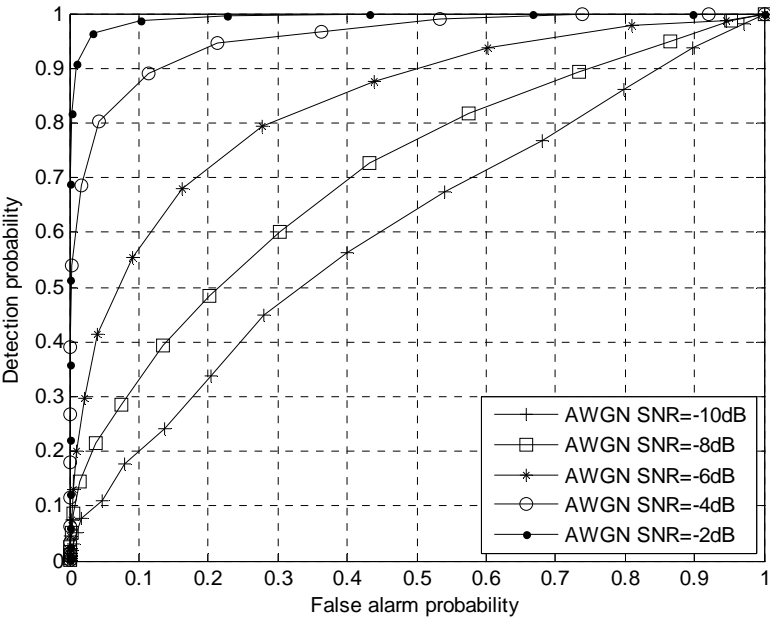


Figure 44: Receiver Operating Characteristic performance of AWGN channel for different SNR values with fixed $N = 1$ and $CP = 1/8$.

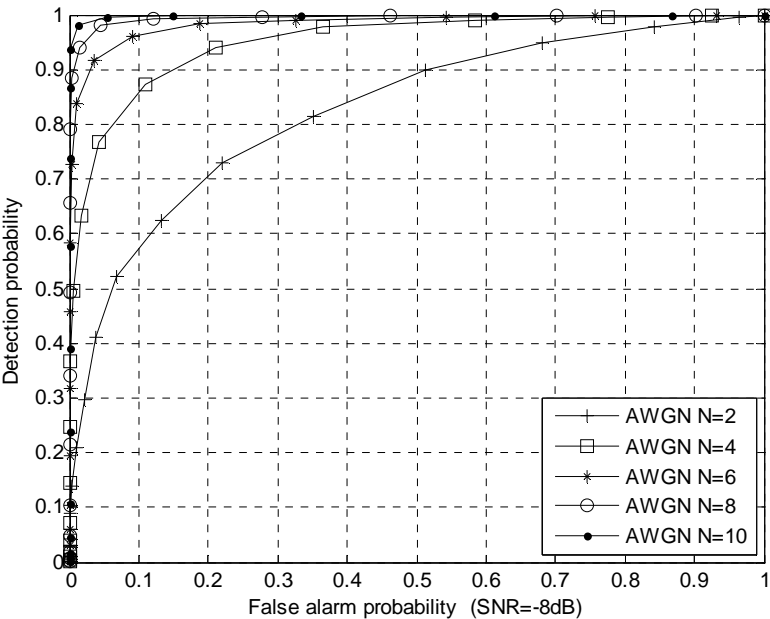


Figure 45: Receiver Operating Characteristic performance of AWGN channel for different N values with fixed $CP = 1/8$ and $SNR = -8$ dB.

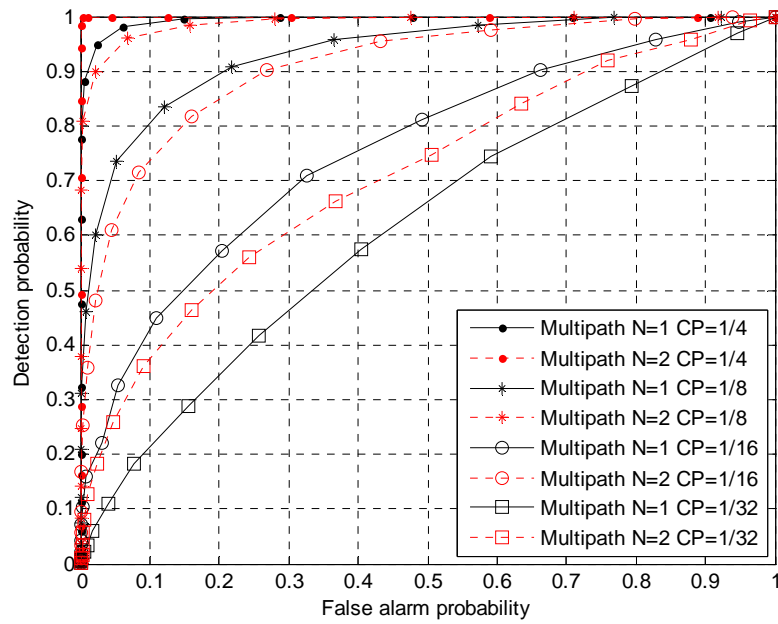


Figure 46: Receiver Operating Characteristic performance of multipath channel for different N and CP values with fixed SNR = -4 dB.

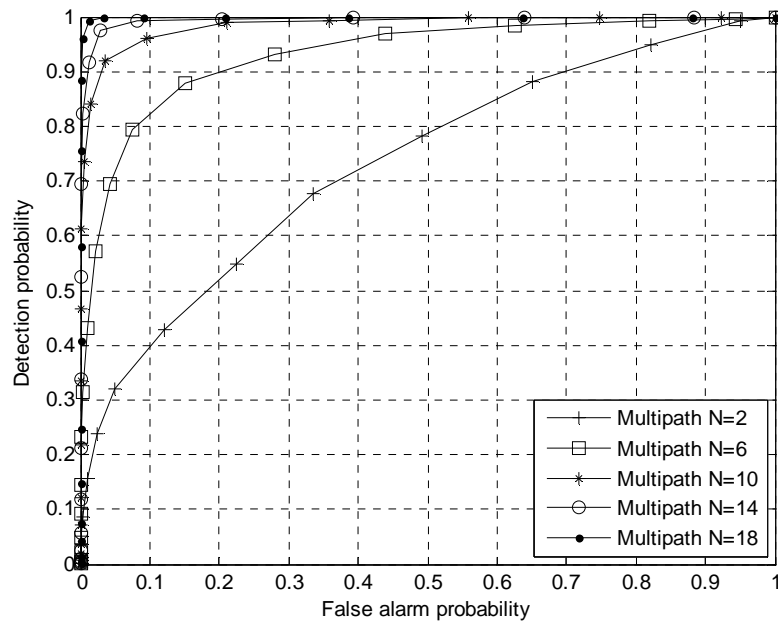


Figure 47: Receiver Operating Characteristic performance of multipath channel for different N values with fixed CP = 1/32 and SNR = -4 dB.

6 Reconfigurability

Dual mode terminals are required in order to ensure compatibility between FBMC and WiMAX, especially at initialization. A possible way to allocate resources to both WiMAX and FBMC is to use different zones for the two types of operation.

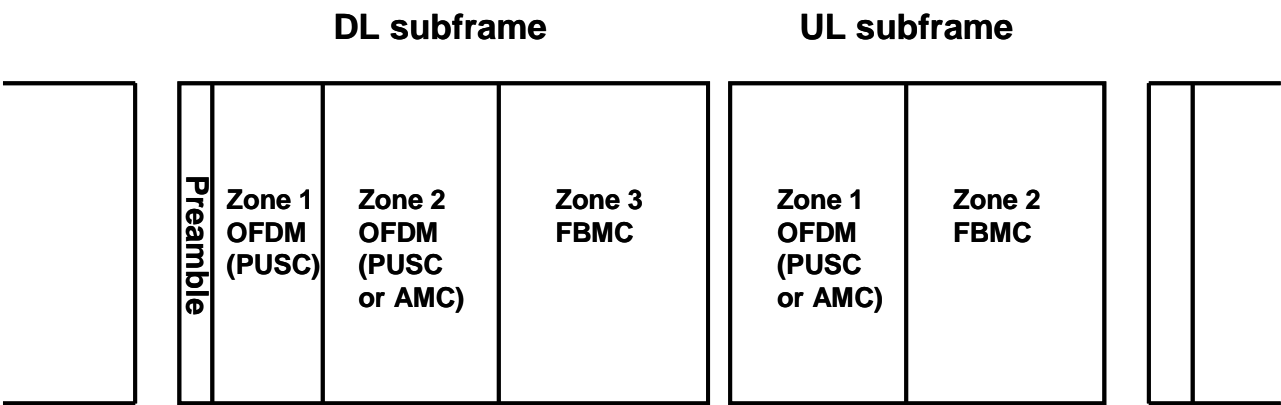


Figure 48: Frame structure for dual mode networks (FBMC zones)

A dual mode station must therefore be able to switch more or less seamless between the two modes. As legacy WiMAX terminals must be able to decode/transmit the frame control structures subframes (Preamble, FCH and MAPs in downlink, ranging and sounding zones in uplink) they must be transmitted in OFDM mode. Thus, as FBMC terminals must be able to decode and transmit these elements used for initialization, either, they need the capability to decode non FBMC signals. Naturally this leads to more complex and especially more expensive FBMC terminals, however, this is necessary, to smoothen the transmission between the physical layers. Thus, a dual mode terminal must be able to operate both in a pure WiMAX network as well as a network serving both WiMAX and FBMC stations. Due to the fact that FBMC and OFDM have strong commonalities the adjustments to be done to the FBMC terminals are not that big. More on this follows later.

Another possible way of introducing FBMC to an existing WiMAX network is the usage of dedicated frames:

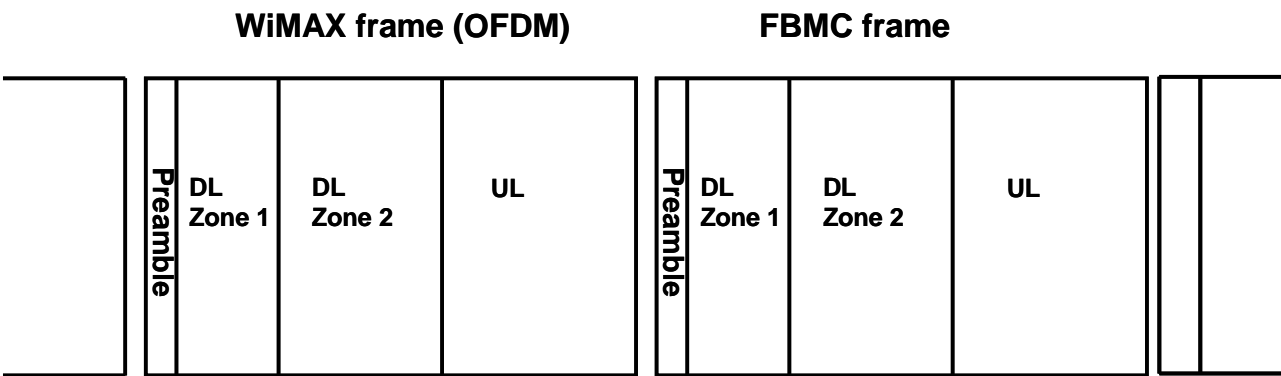


Figure 49: Frame structure for dual mode networks (FBMC frames)

This way FBMC terminals would not necessarily have to be able to decode the WiMAX frames. However, the network entry of WiMAX mobiles may be significantly more error-prone, as it relies on the preamble. There is no way to communicate to terminals, if a specific frame is in OFDM or in FBMC mode, as long as the mobiles have not yet successfully entered the network. For network

entry a mobile typically uses several successive preambles. If FBMC frames are introduced, less OFDM preambles are usable in a given time period. Additionally an OFDM terminal may accidentally try to synchronize onto a FBMC preamble. A possible solution to this problem is to enhance the capability of the mobiles with respect to signal identification. However, existing WiMAX terminals do not have such functionalities and may thus degrade in performance, if a network would switch from pure OFDM mode to the hybrid one. A further possible solution may be to use OFDM preambles even within the FBMC frames. This way network entry of legacy WiMAX terminals would not degrade in performance. However, again the complexity of the FBMC terminals slightly is increased, as OFDM preambles have to be detected.

A logical block diagram of the transmitter is shown in Figure 50. In this figure the blocks that are equal for WiMAX and FBMC are coloured blue. The blocks that have to operate in dual mode are coloured green. The dual mode blocks have to change from WiMAX to FBMC from one zone to the next, which in practice means from one sample to the next.

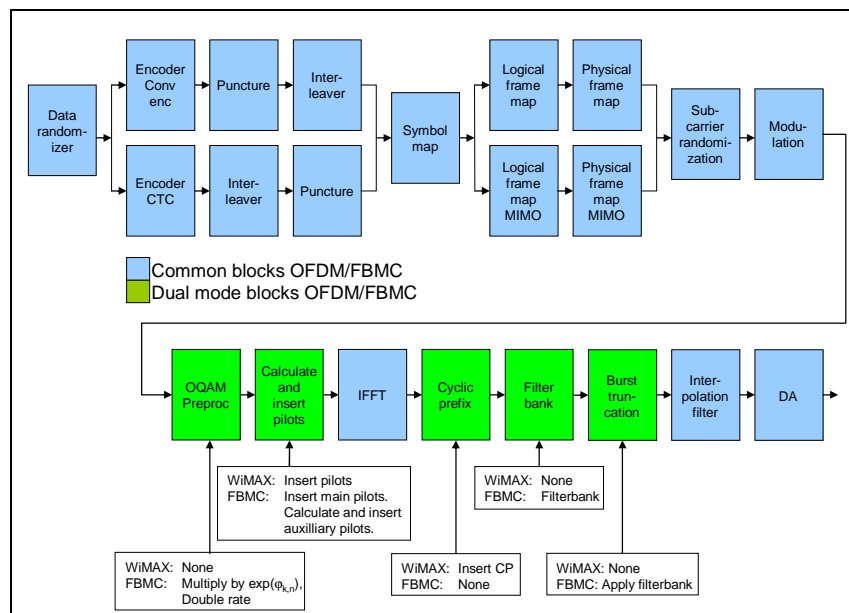


Figure 50: Logical block diagram transmitter

The actual implementation of functions does not necessarily follow the diagram in Figure 50. Several options are possible for the implementation. The test transmitter, which is implemented in WP9, ref Figure 51, is used as an example to show how dual mode operation can be implemented. The physical layer of WiMAX/FBMC is implemented in a Virtex-5 SX 95 FPGA device from XILINX. In a commercial device, however, the actual implementation will be an ASIC and a different design approach will probably be used there.

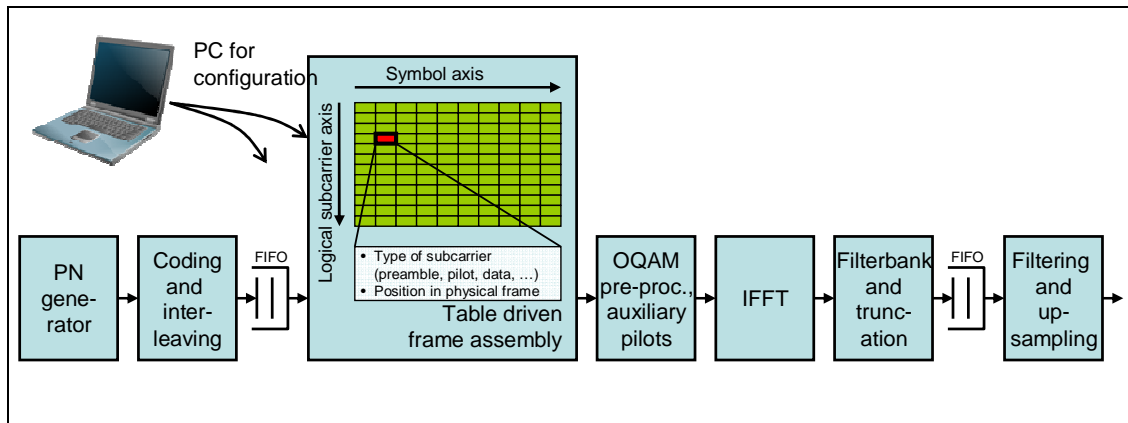


Figure 51: Implementation of WiMAX/FBMC transmitter

The data randomization and FEC are implemented in “hardware”, i.e. shift registers and logical operations on the signal is used. The interleaver is implemented using a memory where the write and read sequences are different.

The frame assembly (symbol map, logical and physical frame map, subcarrier randomization and modulation) uses a table driven approach that can be configured to generate almost any configuration of frame, uplink or downlink for WiMAX and FBMC operation. There is one table element per subcarrier and symbol in the frame. This table element defines the modulation for that subcarrier which can be data (QPSK – 64QAM), a pilot subcarrier or a silent subcarrier. Gain can be set independently for each subcarrier. The table also encodes the logical to physical subcarrier mapping and can implement almost any conceivable mapping. The frame assembly table need not be big enough to hold the entire frame at the same time.

It is up to the MAC layer to calculate the allocation which in turn determines how this table shall be filled with data. This is a task fitted for a programmable device, e.g. an embedded processor. In the demonstrator, which implements only the physical layer of WiMAX/FBMC, this calculation is done in the PC. The allocation and configuration for each user, which determines the content of each subcarrier, is filled into an instruction memory. This instruction memory is large enough to contain an entire frame. The content of this memory is decoded and the different operations are controlled using this decoded information. Just as an illustrative example a block diagram of this machine is shown in Figure 52.

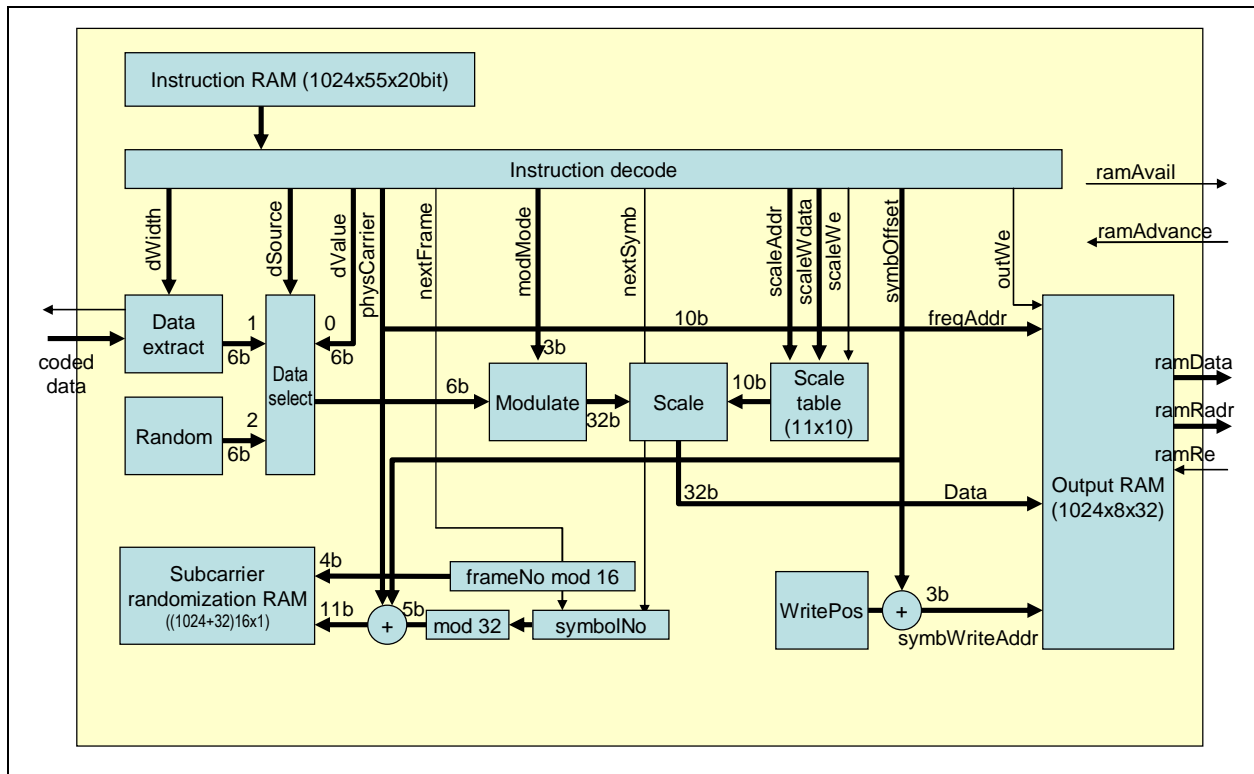


Figure 52: Frame assembly and modulation

The calculation of the auxiliary pilots is done exclusively for FBMC and is done by calculating a linear combination of the surrounding data carriers. The actual implementation of this is done by reading data from the frame assembly memory and calculating the FBMC symbols sequentially. Some elements in the frame assembly table have to be read several times. In WiMAX the same operation can be done but without changing the data. Again, the reading sequence from the frame assembly table and the coefficients for the linear combination of the surrounding samples are calculated in software and loaded into an instruction table such that operation in real time is possible.

The IFFT is equal for both cases except the FBMC requires IFFT calculations at twice the speed. The insertion of the cyclic prefix is done only for WiMAX. The implementation of this function is just a modification of the read sequence of the output memory of the IFFT and this operation comes with almost no hardware cost. For FBMC no cyclic prefix is added.

The structure of the filterbank is shown in Figure 6. The actual implementation of this filter is done by using only two hardware multipliers, one for real part and one for imaginary part. In addition two adders are used. The multipliers and adders are running at 200 MHz clock rate. A memory of size 28 Kbytes is required for the data path (1024 (IFFT size) $\times 7$ (filter length) $\times 16$ bits (wordlength) $\times 2$ (real and imaginary)). The memory size for storing of the filter coefficients is 8 kilobytes (1024 (IFFT size) $\times 4$ (filter length) $\times 16$ bits (wordlength)). The conclusion is that the increase in complexity of the overall hardware is modest when the filterbank is included. When the terminal is operating in WiMAX mode the data flows through the filterbank, but with a coefficient set that disables the filtering function. Zero symbols are filled into the signal path to implement filter preloading. Seamless switching from WiMAX to FBMC mode with filter preloading should be possible using this structure.

Truncation by multiplying the output signal in the time domain by a window function is done after the filterbank. This is a memoryless operation that is done using one multiplier and a window function memory (or possibly a machine calculating the window function on the fly). This function might also be applied to the WiMAX signal in order to reduce out of band radiation.

A concluding remark is that using an FPGA implementation of a WiMAX and FBMC transmitter as a design case, it is possible without any big efforts to implement the transmitter part of a dual mode terminal. In this design it has been a priority to avoid parallel data paths for WiMAX and FBMC. The data flows through the same path and operational mode is controlled by the signal processing methods applied to the signal. These methods are, in our case, controlled by instructions read from a memory or by using different coefficient sets in the filters for the two modes.

The signal processing in the receiver is somewhat more complicated but dual mode operation can be implemented using the same principles. A large part of the transmitter functions have their counterpart in the receiver. The transmitter design can therefore to some extent be reused in the design of a dual mode receiver.

The overall conclusion is that dual mode terminals can be designed with just a modest increase in complexity of the physical layer compared to a pure OFDMA WiMAX terminal.

7 References

- [1] S. Saur, "System Simulation Modelling", PHYDYAS internal document, January 2008.
 - [2] F. Schaich, "WiMAX system profile", PHYDYAS internal document, February 2008.
 - [3] F. Schaich, "Framing in WiMAX", PHYDYAS internal document, February 2008.
 - [4] F. Schaich, "Simulator settings", PHYDYAS internal document, March 2008.
 - [5] F. Schaich, "Ranging, network entry", PHYDYAS internal document, April 2008.
 - [6] F. Schaich, "Residual timing error", PHYDYAS internal document, April 2008.
 - [7] F. Schaich, "Frequency offset in WiMAX", PHYDYAS internal document, April 2008.
 - [8] F. Schaich, "MIMO in WiMAX", PHYDYAS internal document, June 2008.
 - [9] F. Schaich, "Channel estimation", PHYDYAS internal document, June 2008.
 - [10] F. Schaich, "From WiMAX to FBMC", PHYDYAS internal document, July 2008.
 - [11] F. Schaich, "Preamble (DL) and sounding zone (UL)", PHYDYAS internal document, July 2008.
 - [12] F. Schaich, "Burst allocation in WiMAX", PHYDYAS internal document, August 2008.
 - [13] J. Louveaux, L. Baltar, D. Waldhauser, M. Renfors, M. Tanda, C. Bader, E. Kofidis, "Equalization and demodulation in the receiver (single antenna)", ICT-211887 PHYDYAS deliverable D3.1.
 - [14] M. Tanda, T. Fusco, M. Renfors, J. Louveaux, M. Bellanger, "Data-aided synchronization and initialization (single antenna)", ICT-211887, PHYDYAS deliverable D2.1, July 2008.
 - [15] M. Tanda, M. Renfors, J. Louveaux, M. Bellanger, "Synchronization and initialization with single antenna. Blind Techniques.", ICT-211887, PHYDYAS deliverable D2.2, January 2009.
 - [16] P. Cheng, Z. Zhang, X. Zhou, J. Li, P. Qiu, "A Study on Cell Search Algorithms for IEEE 802.16e OFDMA Systems". WCNC 2007, On page(s): 1848-1853, March 2007.
 - [17] H. Li, Y. Bar-Ness, "OFDM Modulation Classification and Parameters Extraction". Cognitive Radio Oriented Wireless Networks and Communications, 2006. 1st International Conference, June 2006. On page(s): 1-6.
 - [18] "PHYDYAS- Physical layer for dynamic spectrum access and cognitive radio", Project website: www.ict-phydyas.org.
 - [19] M. Oner, F. Jondral, "On the Extraction of the Channel Allocation Information in Spectrum Pooling Systems". Selected Areas in Communications, IEEE Journal on Publication Date: April 2007. Volume: 25, Issue: 3. On page(s): 558-565.
 - [20] H. Zhang, D. Le Ruyet, M. Terré, "Signal Detection for OFDM/OQAM System Using Cyclostationary Signatures", IEEE International Symposium on Personal Indoor and Mobile Radio Communications (PIMRC), Sept. 2008, pp. 1-5.
-